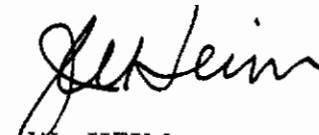## FOREWORD

This study was initiated by the Biophysics Laboratory of the 6570th Aerospace Medical Research Laboratories, Aerospace Medical Division, Wright-Patterson Air Force Base, Ohio. The research was conducted by the Radio Corporation of America, RCA Laboratories, Princeton, New Jersey, under Contract No. AF 33(657)-11336. J. Sklansky was the principal investigator for RCA. H. L. Oestreicher, Chief, Mathematics and Analysis Branch, Biodynamics and Bionics Division, was the contract monitor for the Aerospace Medical Research Laboratories. The work was performed in support of Project No. 7233, "Biological Information Handling Systems and Their Functional Analogs," and Task No. 723305, "Theory of Information Handling." The research for this report was performed between May 1963 and October 1963.

ABSTRACT

In certain "threshold learning processes" (TLPs) associated with pattern recognition and sensory perception, the process of training an observer to recognize patterns or distinguish levels of sensory excitation may be modeled by a finite-state Markov chain. When the statistics of the signals received by the observer move at random between two sets of parameters, we have a "two-mode" TLP, modeled by a two-mode Markov chain. Using a probabilistic measure of effectiveness, the effectiveness of a "simple incremental" feedback policy is shown to be greater for two-mode TLPs than for one-mode TLPs over a certain range of environmental and structural statistics. A method of designing periodic train-work schedules for two-mode TLPs is described. ("Train" and "work" correspond to "closed-loop" and "open-loop" respectively.) In many real adaptive processes an "RC approximation" of the train-work dynamics is applicable. For these processes the ratio of working time to retraining time, yielding a desired performance level, is maximized when the work-retrain period is made as small as possible. Many stochastic processes present modeling problems of near psychological complexity. Ways in which open-loop/closed-loop relationships can help the life scientist or engineer model adaptive stochastic processes by two-mode TLPs are indicated.

PUBLICATION REVIEW

This technical documentary report is approved.

J. W. HEIM
Technical Director
Biophysics Laboratory

iii

LIST OF TABLES

LIST OF SYMBOLS

SYMBOL	MEANING OF SYMBOL
$\underline{r}$	Row vector. In some cases $\underline{r}$ is a column vector — this will be clear from the context.
$\underline{r}(n)$	Row vector as a function of n.
$\underline{\underline{r}}(n)$	x-transform of $\underline{r}(n)$
n	An integer representing *time* or *number of trials*.
$\underline{\underline{M}}$	A matrix.
$\underline{M}(n)$	A matrix-valued function of n.
$\underline{\underline{M}}(x)$	x-transform of $\underline{M}(n)$.
$\underline{\underline{\triangle}}$	Is defined equal to.

I. INTRODUCTION

We are studying the effect of various forms of feedback on the adaptation characteristics [ref. 1] of adaptive processes in the life sciences and man-machine interactions. We are also searching for open-loop/closed-loop relationships in various stochastic models that will help us explain the adaptive behavior of life processes in terms of simple feedback mechanisms.

Here we report a few results of a study of a simple form of threshold feedback as a training policy for "two-mode" stochastic processes. Two-mode stochastic processes are stochastic processes whose statistical parameters are themselves subject to statistical fluctuation. Specifically, these parameters fluctuate at random between two sets of values. Two-mode stochastic processes are inherently more difficult to train than one-mode stochastic processes. This difficulty is reflected in terms of a need for periodic retraining, which is not needed in one-mode processes. On the other hand the effectiveness of feedback as a means for overcoming environmental and structural fluctuations seems to be greater for two-mode processes than for one-mode processes.

Among the results of this study are certain open-loop/closed-loop relationships that show promise of helping us choose the best lengths of the training and working periods.

Our initial research has focused on adaptive signal detection in psychology and communication systems. In the future we shall select other particular processes in the life sciences and engineering, and we shall show how our understanding of the mathematics of feedback and adaptation can: (a) help construct models of these processes, and (b) suggest new experiments toward enhancing our understanding of adaptation.

MAJOR CONCEPTS AND DEFINITIONS

In this section we shall sketch a few of the major concepts in our research, and present a few definitions.

Adaptation Characteristics, Learning, Self-Healing: Many biological processes as well as man-made processes are often described as "adaptive" in some sense. Since adaptive seems to mean so many different things to different people, we present our view of the meaning of this term. When a process is adaptive, we mean that it exhibits certain invariances in its behavior in response to fluctuations in its environment and its internal structure. Specifically, an adaptive process will exhibit the following *adaptation characteristics* [ref. 1]:

Stability: The performance index remains within prescribed bounds when the environment changes.

Reliability: The performance index remains within prescribed bounds when the internal structure changes.

Learning may be viewed as a favorable time variation of the performance index when the environment undergoes a step transition. *Self-healing* may be viewed as a favorable time variation of the performance index when the internal structure undergoes a step transition. Thus learning may be viewed as a facet of stability, and self-healing as a facet of reliability.

Ignorance: Any discussion of adaptive processes must deal with the concept of ignorance. The engineer's ignorance of the precise nature of a machine's future task forces him to design

1

machines that will adapt to fluctuations in environment and internal structure. In biological processes these fluctuations are greater in complexity than in man-made systems, and the adaptive power of biological processes is correspondingly greater. When we use the term "ignorance," then, in our discussions of adaptive processes, we are referring to these unpredictable environmental and structural fluctuations.

In an earlier paper, we dealt with a class of processes in which the ignorance of the environment and the structure was expressed by a stationary pair of "constituent" probability densities [ref. 2]. In the present paper we expand the scope of the ignorance by introducing the two-mode stochastic process, in which the parameters of the constituent densities are themselves subject to random fluctuation. This increases the amount of training needed to achieve a required performance level, but it also increases the effectiveness of feedback as a means of accommodating unpredictable events.

Plant: When the feedback loop of an adaptive process is removed, the system that remains is called an open-loop process or "plant." The plant denotes that part of a system which is being trained by the feedback loop.

Stochastic Process: In many adaptive processes, ignorance of the stimulus environments and of the behavioral characteristics of the plants is conveniently described in terms of probabilistic or stochastic models. Examples occur in pattern recognition, communication systems, human and animal learning, and randomly disturbed control systems. We take the liberty of calling the processes themselves stochastic, even though only the models are truly stochastic.

We view feedback as a means of enhancing the stability and/or reliability of a biological process or a manmade machine. The feedback may appear as an explicit deterministic manmade mechanism, such as the reinforcement policies in the simple learning tasks of the "stochastic-models-of-learning" school of psychology; or it may appear as an implicit natural mechanism, such as the apparent strengthening of neural firing mechanisms in response to frequency of use. In either case, feedback is usually a deterministic mechanism, in contrast to the plant, which is usually described stochastically. The reason for the stochastic description of the plant is twofold: (1) our ignorance of the plant and its environment is often conveniently expressed by probabilities, and (2) the mathematics of certain stochastic models is convenient and suggestive.

Mode: In some stochastic processes, it is convenient to assume that the statistical parameters of the models are themselves subject to statistical fluctuation. Here we have one stochastic model superimposed on another stochastic model.

Under what circumstances is such a hypothesis warranted? The hypothesis seems warranted whenever the measured statistical parameters seem to jump to new values very suddenly, and to remain at those values over a period of time substantially longer than the interval used for estimating these parameters. This situation occurs frequently in communication systems, and is explained by bursts of noise entering or leaving the channel [ref. 3]. We shall refer to such processes as two-mode stochastic processes. When the statistics of a process are constant, we shall call the process one-mode or stationary.

Each mode of a two-mode process is a one-mode process whose statistical characteristics may be determined by fixing the statistical parameters of the environment at one of the two sets of values. If such a fixing is not physically possible or practical, it might be achieved by a computer simulation of the environment.

2. ANALYSIS OF TWO-MODE ADAPTIVE PROCESSES

Consider a plant in which a binary signal is transmitted through a two-mode channel. If the channel is fixed in mode A, it acts as a zero-memory channel with relatively good transmission statistics. If the channel is fixed in mode B, it acts as a different zero-memory channel with relatively bad transmission statistics. In a one-mode operation, i.e., in the case where the channel is fixed at either mode A or mode B, the transmission statistics are stationary. In the two-mode operation, the channel is only temporarily fixed at either A or B, and the transmission statistics follow a random square wave as a function of time, such as the uppermost wave in Figure 1. In the model to be discussed, the transitions between A and B are described by a Markov chain, as indicated in Figure 2. This model is a generalized version of the burst-noise channel described by E. N. Gilbert [ref. 3].
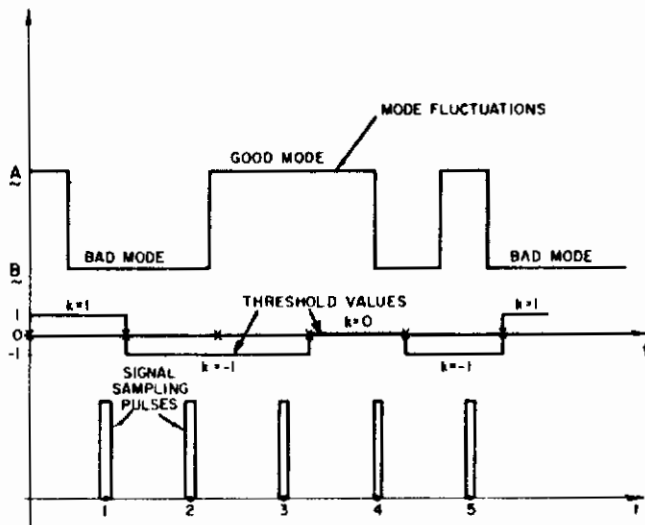
Figure 1. Timing Relations between Mode-to-Mode Transitions, Threshold Shifts, and Sampling Pulses.

Figure 2. State Transition Graph of the Mode-to-Mode Behavior of a Two-Mode Process.
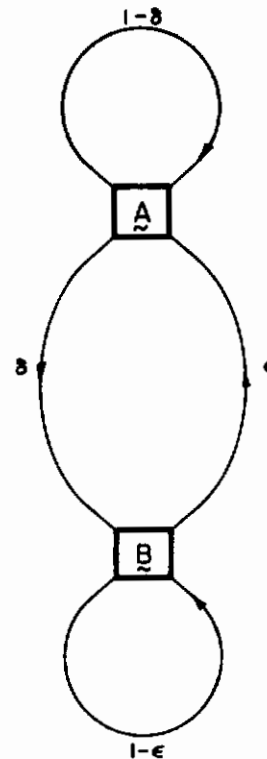
Now suppose the plant is trained by a simple incremental feedback policy. In this feedback policy the controlled variable is a threshold having K possible values: $k = 1, 2, ..., K$. The threshold is moved up or down in response to a false alarm or false rest, respectively. The threshold remains fixed if no error is incurred or if a boundary threshold prevents a desired adjustment. This feedback· policy is discussed in detail in an earlier paper, where it is referred to as the simple-TLP rein-forcement policy [ref. 2]. In this report we refer to it as the simple-incremental feedback policy.

As a result of this feedback, each mode is describable as a random walk of the form shown in Figure 3. (In Figure 3, K is 3.)
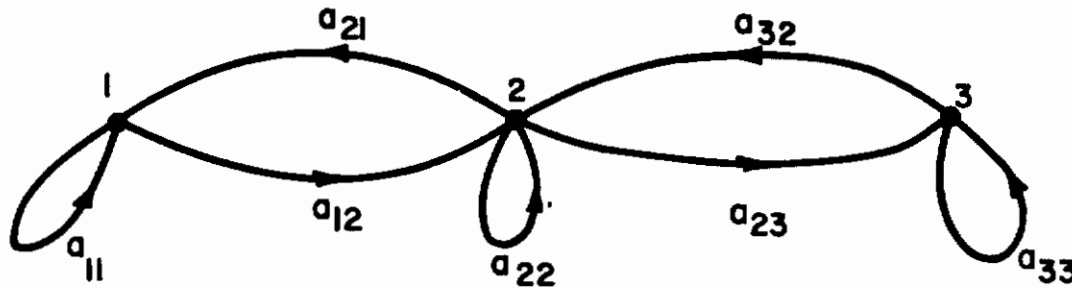
Figure 3. The Random Walk Description of a One-Mode TLP with a
Simple Incremental Feedback Policy.

Note that the two-mode process is a special case of the situation where each transition probability of a Markov chain shifts unpredictably from one value to another. We shall see that such an apparently complicated model is, in the case of a two-mode (or N-mode) Markov chain, actually equivalent to a Markov chain with constant transition probabilities. Thus a stationary Markov chain can be used as a model of a certain class of processes having nonstationary environmental statistics!

The following question now arises: How may the two-mode process be described in terms of the individual mode matrices

$$\underline{A} \overset{\Delta}{=} \{a_{ij}\}, \quad \underline{B} \overset{\Delta}{=} \{b_{ij}\} \tag{1}$$

and the mode-to-mode transition matrix

$$\Gamma \overset{\Delta}{=} \begin{bmatrix} 1-\delta & \delta \\ \epsilon & 1-\epsilon \end{bmatrix} ? \tag{2}$$

The specific answer to this question depends on the way in which the states of the two-mode Markov chain are defined. We shall define these states as follows. Let A1, A2, A3, B1, B2, B3 denote the six states of a two-mode Markov chain in which the constituent modes each have three thresholds. (The extension to modes of more than three thresholds will be obvious.)

Now consider the sequence of events illustrated in Figure 1. These events refer to the guesses and the error signals generated in a three-threshold TLP (for Threshold Learning Process). The block diagram of a TLP is given in Figure 4. Just before the observer in Figure 4 generates a guess, he receives a sampling pulse which tells the observer: during this sampling interval guess whether the observed signal, v, was caused by a 0 or a 1 at the information source. During the sampling interval the channel will be either in mode $\underline{A}$ or mode $\underline{B}$. If it is in $\underline{A}$, then

4
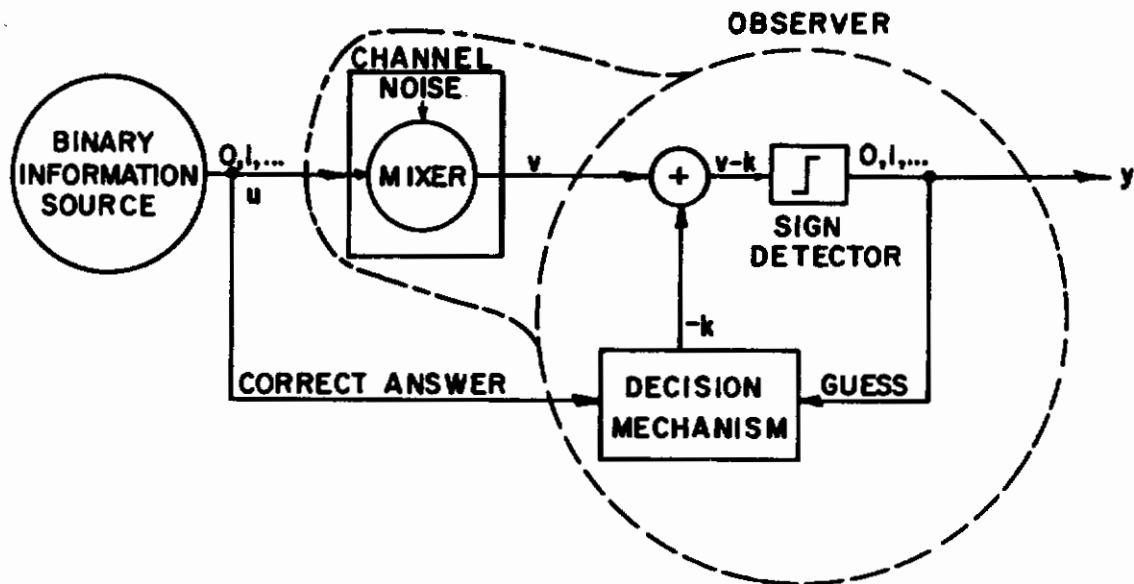
Figure 4. Block Diagram of a TLP

the two-mode process is said to be in the state Ak from the time that the threshold takes on the value k chosen by the decision mechanism until the next time a threshold value is established. (The next established threshold value may or may not be different from the "present" value.) Similarly, if the channel is in mode $\underset{\sim}{B}$ during the sampling pulse then the next state of the two-mode process will be Bk, where the increment in k depends on the size and sign of the error. Note that by this definition of Ak and Bk, the model of the process may occupy state Ak even though the process itself may have shifted to $\underset{\sim}{B}$. Similarly the model may be in state Bk even though the channel is in $\underset{\sim}{A}$. The reason for the proposed definition is the nonambiguity and simplicity of the resulting mathematical analysis. Actually, no loss of generality is imposed by the definition. (A definition by which the model is in state Ak if and only if the channel is in $\underset{\sim}{A}$ at the time of threshold adjustment results in an ambiguous mathematical formulation, which we shall come back to later.)

By the above definition, a transition from states Ai to Bj occurs with probability δb_{ij}, Bi to Bj occurs with probability $(1-\epsilon)b_{ij}$, Ai to Aj occurs with probability $(1-\delta)a_{ij}$, and Bi to Aj occurs with probability ϵa_{ij}. Consequently the process may be described by the signal flow graph of Figure 5b. [See ref. 4.] In part a of Figure 5 is a signal flow graph displaying only the mode-to-mode transitions. (The quantity x in these graphs represents a unit-delay operator.) To help us in our analysis, the graph of Figure 5b may be represented by a "vector flow graph" each of whose nodes represents a vector having state probabilities as elements, and each of whose branches represents a matrix operating on the node vector at the tail of the branch. A convenient partition of the state probabilities into vectors is $\underline{r}_A(n)$ and $\underline{r}_B(n)$, where the elements of $\underline{r}_A(n)$, $\underline{r}_B(n)$ are the probabilities of states Ak, Bk, respectively, for k = 1, 2, 3. The resulting vector flow graph is shown in Figure 6. The stimulus-response equations are obtainable in matrix form directly from this graph. This matrix equation is:

$$
\left[\underline{r}_A(x), \ \underline{r}_B(x) \right] = \left[\underline{s}_A(x), \ \underline{s}_B(x) \right] + \left[\underline{r}_A(x), \ \underline{r}_B(x) \right]
\begin{bmatrix}
(1-\delta)\underline{A} & \delta\,\underline{B} \\
\epsilon\,\underline{A} & (1-\epsilon)\underline{B}
\end{bmatrix} x.
\tag{3}
$$

where $\underline{s}_A(x)$, $\underline{r}_A(x)$, etc. are x-transforms of stimulus probabilities and response probabilities.

5
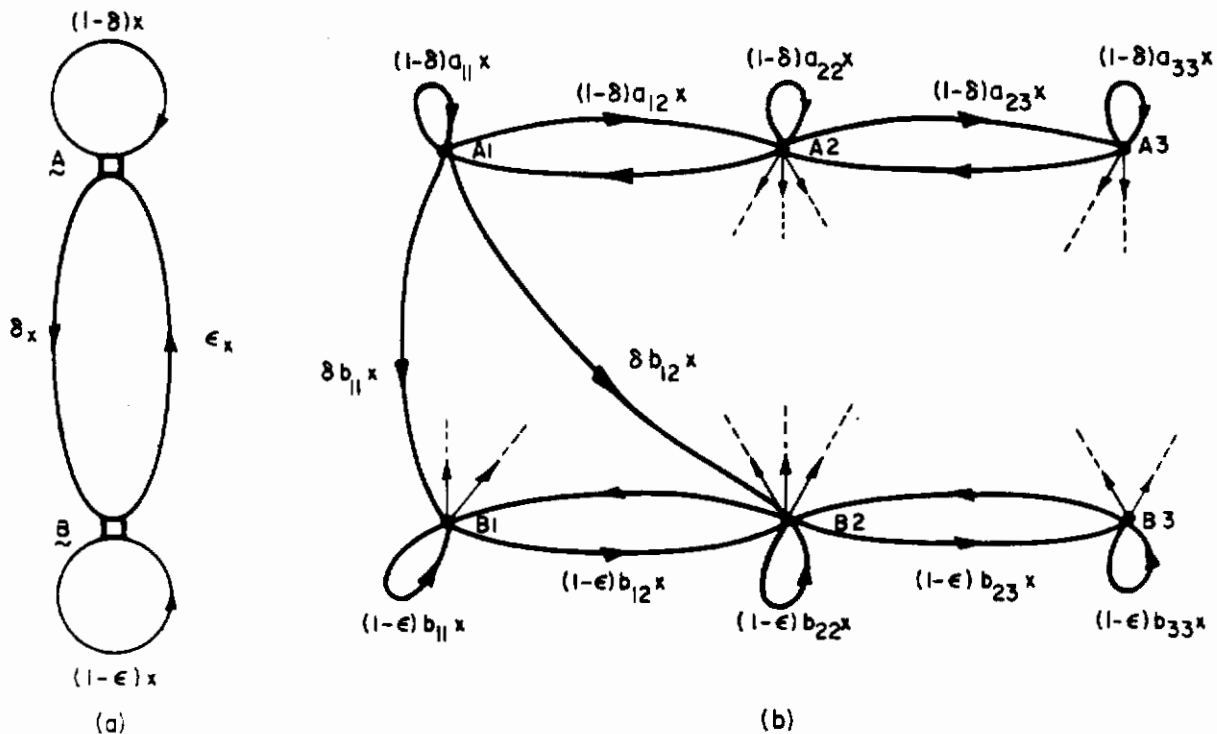
Figure 5. Markov Chain Model of a Two-Mode Process.
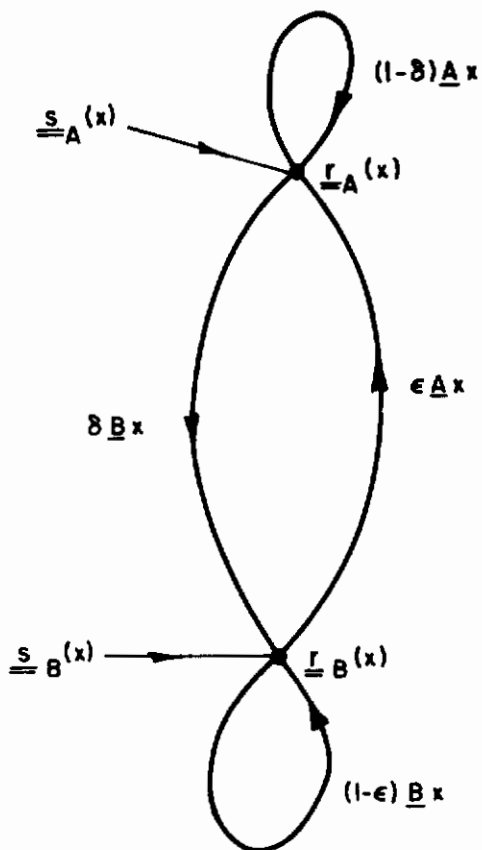
Figure 6. The Vector Flow Graph of a Two-Mode Markov Chain.

6

Let

$$\underline{r}(x) \stackrel{\Delta}{=} \left[\underline{r}_A(x), \ \underline{r}_B(x)\right] \tag{4}$$

$$\underline{s}(x) \stackrel{\Delta}{=} \left[\underline{s}_A(x), \ \underline{s}_B(x)\right] \tag{5}$$

$$\underline{\underline{\Gamma}} \stackrel{\Delta}{=} \begin{bmatrix} 1-\delta & \delta \\ \epsilon & 1-\epsilon \end{bmatrix} \tag{6}$$

$$\underline{\underline{P}} \stackrel{\Delta}{=} \begin{bmatrix} \underline{A} & 0 \\ 0 & \underline{B} \end{bmatrix} \tag{7}$$

Then Equation 7 may be written in the form

$$\underline{r}(x) = \underline{s}(x) + \underline{r}(x)\,\underline{\Gamma}\,\underline{P}\,x. \tag{8}$$

Hence the general stimulus-response equation is

$$\underline{r}(x) = \underline{s}(x)\left[\underline{I} - \underline{\Gamma}\,\underline{P}\,x\right]^{-1} \tag{9}$$

If $\underline{s}(x)$ is the x-transform of an impulse vector, i.e., a vector each of whose elements is an impulse, then

$$\underline{s}(n) = \{r_i(0)\ \delta(0,n)\} \ \text{and} \tag{10}$$

$$\underline{r}(n) = \underline{r}(0)\,(\underline{\Gamma}\ \underline{P})^n. \tag{11}$$

Note that $(\Gamma\ P)^n \neq \Gamma^n\,P^n$, because $\underline{\Gamma}\ \underline{P} \neq \underline{P}\ \underline{\Gamma}$, except in trivially degenerate cases.

DISADVANTAGES OF A DIFFERENT DEFINITION OF THE STATE OF THE PROCESS

Suppose we had defined "state" as follows: The process occupies state Ak if and only if the channel is in mode $\underline{A}$ at the instant immediately following a threshold transition, the value of k identifying the threshold existing at that instant. In this case we would have to consider two classes of transition probabilities: class 1 referring to those cases in which no change of mode occurs in the interval after the sampling pulse and before the threshold adjustment, and class 2 referring to those cases in which such a change of mode does occur. Class 1 leads to Equation 9 as the stimulus-response equation for the process. But class 2 leads to a stimulus-response equation in which the order of $\underline{\Gamma}$ and $\underline{P}$ is reversed, namely:

$$\underline{r}(x) = \underline{s}(x)\ \left[I - \underline{P}\ \underline{\Gamma}\ x\right]^{-1} \tag{12}$$

This situation is ambiguous, because we cannot predict when class 1 or class 2 will occur. Additional data on the occurrence probabilities of classes 1 and 2 is needed in order to resolve the ambiguity. Even if the ambiguity is resolved, the mathematical formulation still will be substantially less tractable than that resulting from the first definition of "state."

Our analysis of two-mode adaptive processes — in particular, two-mode TLPs — is focused on two types of operation: the training phase and the working phase. In the training phase the feedback loop in Figure 4 is closed. In the working phase the feedback loop is open, so that the threshold k is fixed. Thus training and working correspond directly to closed-loop and open-loop, respectively.

3. THE TRAINING PHASE

We shall now derive an expression for the success probability, $z(n)$, as a function of time, n, in response to an impulse vector. (An impulse vector corresponds to the situation where the initial thresholds have a fixed initial distribution.) This quantity is a measure of success as a function of the length of training.

Equation 3 can be solved for $\underline{r}_A(x)$ by treating it as two simultaneous matrix equations, and replacing $\underline{r}_B(x)$ by an expression involving $\underline{r}_A(x)$ and *not* involving $\underline{r}_B(x)$. This yields

$$\underline{r}_A(x) = \left\{ \underline{s}_A(x) + \underline{s}_B(x) \left[I - (1-\epsilon)\,\underline{B}x \right]^{-1} \epsilon \underline{A}x \right\} \underline{\underline{M}}(x) \tag{13}$$

where

$$\underline{\underline{M}}(x) \overset{\Delta}{=} \left\{ [\underline{I} - (1-\epsilon)\,\underline{B}x][\underline{I} - (1-\delta)\cdot\underline{A}x] - \delta\epsilon\underline{\underline{B}A}x^2 \right\}^{-1} [\underline{I} - (1-\epsilon)\underline{B}x] \tag{14}$$

Similarly,

$$\underline{r}_B(x) = \left\{ \underline{s}_A(x) \left[I - (1-\delta)\,\underline{A}x \right]^{-1} \delta\underline{B}x + \underline{s}_B(x) \right\} \underline{N}(x) \tag{15}$$

where

$$\underline{N}(x) \overset{\Delta}{=} \left\{ [I - (1-\delta)\underline{A}x][I - (1-\epsilon)\,\underline{B}x] - \delta\epsilon\underline{AB}x^2 \right\}^{-1} [I - (1-\delta)\,\underline{A}x] \tag{16}$$

Suppose the training process starts with the initial threshold at $k = 1$. We may analyze this training process by setting

$$\underline{s}(x) = \left[\underline{r}_A(0),\ \underline{r}_B(0) \right] \tag{17}$$

where

$$\underline{r}_A(0) = \frac{\epsilon}{\delta+\epsilon}\ [1, 0, 0], \qquad \underline{r}_B(0) = \frac{\delta}{\delta+\epsilon}\ [1, 0, 0]. \tag{18}$$

The coefficients $\epsilon/(\delta+\epsilon)$, $\delta/(\delta+\epsilon)$ represent the asymptotic probability that the channel modes will be $\underline{A}$, $\underline{B}$, respectively. (We assume in our analysis that the mode-to-mode fluctuations have reached steady-state statistics.)

More generally, the training process will start with an initial probability distribution over the range of available thresholds. For this case we have

$$\underline{s}_A(x) = \underline{r}_A(0) = \gamma\underline{r}(0), \text{ and } \underline{s}_B(x) = \underline{r}_B(0) = (1-\gamma)\ \underline{r}(0), \tag{19}$$

where

$$\gamma \overset{\Delta}{=} \frac{\epsilon}{\delta+\epsilon}\ , \tag{20}$$

and where $\underline{r}(0)$ is a probability vector, i.e., a vector having non-negative real elements summing

8

to unity. For this situation, Equations 13, 15, 17, and 19 yield

$$\underline{r}_A(x) = \underline{r}(0)\left\{\gamma\underline{I} + (1-\gamma)\left[\underline{I} - (1-\epsilon)\underline{B}x\right]^{-1}\epsilon\underline{A}x\right\}\underline{M}(x) \tag{21}$$

$$\underline{r}_B(x) = \underline{r}(0)\left\{(1-\gamma)\underline{I} + \gamma\left[\underline{I} - (1-\delta)\underline{A}x\right]^{-1}\delta\underline{B}x\right\}\underline{N}(x) \tag{22}$$

Now, the success probability $z(n)$ may be found from the following formula*:

$$z(n) = \underline{r}_A(n)\,\underline{q}_A + \underline{r}_B(n)\,\underline{q}_B \tag{23}$$

where $\underline{q}_A \overset{\Delta}{=}$ a column vector of conditional success probabilities for states in mode $\underset{\sim}{\text{A}}$

$\underline{q}_B \overset{\Delta}{=}$ a column vector of conditional success probabilities for states in mode $\underset{\sim}{\text{B}}$.

(Note that since $\underline{q}_A$ and $\underline{q}_B$ are column vectors, the terms $\underline{r}_A(n)\,\underline{q}_A$ and $\underline{r}_B(n)\,\underline{q}_B$ represent inner products [ref. 5].)

When $z(n)$ is plotted as a function of time, we have what might be called a "learning curve." In order to avoid controversy over semantics, however, we shall refer to it as a performance wave, and point out that our performance wave is the learning curve as defined by certain schools of psychology.

The vectors $\underline{q}_A$ and $\underline{q}_B$ are obtainable from an inspection of the state transition graph (or signal flow graph, such as Figure 5b) and from a knowledge of the "boundary success probabilities" p_{A1}, p_{A3}, p_{B1}, p_{B3}. We define p_{A1} as the probability of success on the "next" trial, given that the present threshold is $k = 1$ and that the present mode is A. The remaining boundary success probabilities are defined in a similar fashion.

Example:

Let
$$\underline{q}_A \overset{\Delta}{=} (q_{A1},\ q_{A2},\ q_{A3}) \tag{24}$$

Then, an inspection of Figure 5b yields

$$\left.\begin{aligned}
q_{A1} &= (1-\delta)\,a_{11}\,p_{A1} + \delta b_{11}\,p_{B1} \\[2mm]
q_{A2} &= (1-\delta)\,a_{22} + \delta b_{22} \\[2mm]
q_{A3} &= (1-\delta)\,a_{33}\,p_{A3} + \delta b_{33}\,p_{B3}
\end{aligned}\right\} \tag{25}$$

The vector $\underline{q}_B$ may be found in a similar fashion.

The x-transform of $z(n)$ follows from an x-transformation of Equation 23:

$$\underset{\sim}{z}(x) = \underline{r}_A(x)\,\underline{q}_A + \underline{r}_B(x)\,\underline{q}_B\,. \tag{26}$$

---

*In an earlier paper [ref. 2] we used a slightly different time origin for $z(n)$. By the definition for $z(n)$ in that paper, the variable n in the left member of Equation 23 would be replaced by $n+1$. The change in time origin is just a matter of convenience.

9

In conjunction with Equations 13 and 15, Equation 26 gives us an exact formula for $\underset{\sim}{z}(x)$. If the initial threshold probability vector is $\underline{r}(0)$, then Equations 21 and 22 may be used in place of Equations 13 and 15.

We may think of the mode-to-mode transitions as "slow" or "fast," depending on the size of δ and ϵ. Slow transitions correspond to $\delta \ll 1$ and $\epsilon \ll 1$. Fast transitions correspond to $1 - \delta \ll 1$ and $1 - \epsilon \ll 1$. In the differential-equation analysis of adaptive control systems, systems with fast plant variations have not been satisfactorily analyzed, and systems with slow plant variations have yielded only to approximate analysis. The present approach permits an exact analysis of both slowly and rapidly perturbed systems.

Later in this report we shall refer to two-mode processes having slow mode-to-mode transitions as weakly coupled processes, borrowing a term from electrical engineering. When δ and ϵ are large, the process will be called strongly coupled.

PEAK SETTLING TIME OF TRAINING PERFORMANCE WAVES

We define the *peak settling time* $\hat{N}$ of the training performance waves of two-mode TLPs as follows:

$$\hat{N} \overset{\Delta}{=} \underset{z(0)}{\text{Max}} \; N[z(0)] \tag{27}$$

where $N[z(0)]$ is the smallest positive integer satisfying

$$|z(m) - z(0)| \geq 0.9 \, | \, \zeta - z(0) \, | \text{ for all } m \geq N[z(0)] . \tag{28}$$

This definition is identical to that for one-mode processes given in an earlier paper [ref. 2]. (See footnote on page 9). In that paper we found that a good estimate of $\hat{N}$ is given by

$$\hat{N} \cong \nu \overset{\Delta}{=} \log_\xi 10 \tag{29}$$

where ξ is the eigenvalue closest to but not on the unit circle of the x-plane.

Later we shall give an example of the use of ν in the estimation of the training performance wave of a specific two-mode process.

APPROXIMATION FOR WEAKLY COUPLED PROCESSES

When the process is weakly coupled, i.e., when the mode-to-mode fluctuations are slow, we have $\delta \ll 1$, $\epsilon \ll 1$. For this case, Equations 13 and 15 reduce to

$$\underline{r}_A(x) \cong \underline{\underline{s}}_A(x) \, [\underline{I} - Ax]^{-1} \tag{30}$$

$$\underline{r}_B(x) \cong \underline{\underline{s}}_B(x) \, [\underline{I} - \underline{B}x]^{-1} \tag{31}$$

assuming $\underline{\underline{s}}_A(x)$ and $\underline{\underline{s}}_B(x)$ are comparable in magnitude. For the simple training process, $\underline{\underline{s}}_A(x)$ and $\underline{\underline{s}}_B(x)$ are given by Equation 19. For this situation, we have

10

$$\underline{r}_A(x) \cong \gamma \, \underline{r}(0) \, [\underline{I} - \underline{A}x]^{-1} \qquad (32)$$

and

$$\underline{r}_B(x) \cong (1 - \gamma) \, \underline{r}(0) \, [\underline{I} - \underline{B}x]^{-1} \qquad (33)$$

Consider the one-mode process $\underline{A}$. Suppose the initial threshold distribution is $\underline{r}(0)$. Then the training threshold probability is given *exactly* by the following formula [ref. 2]:

$$\underline{r}_{Ao}(x) = \underline{r}(0) \, [\underline{I} - \underline{A}x]^{-1} \qquad (34)$$

Similarly,

$$\underline{r}_{Bo}(x) = \underline{r}(0) \, [\underline{I} - \underline{B}x]^{-1} \qquad (35)$$

(The subscripts Ao and Bo stand for "$\underline{A}$ only" and "$\underline{B}$ only.") Hence, by Equations 32 and 33, the two-mode threshold probabilities during training are approximately proportional to the corresponding one-mode threshold probabilities:

$$\underline{r}_A(x) \cong \gamma \, \underline{r}_{Ao}(x)$$

$$\underline{r}_B(x) \cong (1 - \gamma) \, \underline{r}_{Bo}(x)$$

Now consider the conditional success probabilities for the one-mode process $\underline{A}$. From Figure 3 we obtain

$$q_{Ao1} = a_{11} \, p_{A1}, \qquad q_{Ao2} = a_{22}, \qquad q_{Ao3} = a_{33} \, p_{A3} \, . \qquad (36)$$

Comparing Equations 36 and 25, we note that

$$\left. \begin{array}{l} \underline{q}_A = (1 - \delta) \, \underline{q}_{Ao} + \delta \, \underline{q}_{Bo} \\[2mm] \underline{q}_B = \epsilon \, \underline{q}_{Ao} + (1 - \epsilon) \, \underline{q}_{Bo} \end{array} \right\} \qquad (37)$$

These equations are applicable to all two-mode TLPs, independently of the number of thresholds, even though Figure 3 has only three thresholds. Note that

$$\underline{q}_A \cong \underline{q}_{Ao} \quad \text{when} \quad \delta \ll 1 \qquad (38)$$

and

$$\underline{q}_B \cong \underline{q}_{Bo} \quad \text{when} \quad \epsilon \ll 1 \, . \qquad (39)$$

Now,

$$\underline{z}_{Ao}(x) = \underline{r}_{Ao}(x) \, \underline{q}_{Ao} \qquad (40)$$

$$\underline{z}_{Bo}(x) = \underline{r}_{Bo}(x) \, \underline{q}_{Bo} \qquad (41)$$

11

Hence, for $\delta \ll 1$ and $\epsilon \ll 1$,

$$\underset{\sim}{z}(x) \cong \gamma \, z_{A_0}(x) + (1 - \gamma) \underset{\sim}{z}_{B_0}(x). \tag{42}$$

An inverse x-transformation of this equation yields

$$z(n) \cong \gamma \, z_{A_0}(n) + (1 - \gamma) \, z_{B_0}(n). \tag{43}$$

for $\delta \ll 1$, $\epsilon \ll 1$.

Under the Two-Mode Example — Part 2 on page 35, we shall indicate the size of the errors encountered in the use of the above approximation. We shall see that when the approximation holds good at $n = \infty$, it will hold good for the entire range of n between zero and infinity. We shall see in the example that the error in the approximation increases monotonically with increasing n, approaching a constant asymptote as $n \to \infty$.

A general error analysis for Equation 43 has not been developed. Such an analysis would provide a useful supplement to the present work.

INFINITE TRAINING

After a long training interval, the success probability of the two-mode process approaches an asymptote ζ. We would like to obtain a closed-form expression for ζ in terms of the one-mode matrices $\underline{A}$ and $\underline{B}$ and the mode-to-mode transition probabilities δ and ϵ. A direct approach to obtaining such an expression is to find the residues at $x = 1$ of Equations 21 and 22. Because of the complexities involved in finding these residues, we have not obtained the desired expression.

A weak-coupling approximation, however, is easy to obtain. We have seen that a good approximation for $z(n)$ is given by Equation 43. Taking the limit of this equation as $n \to \infty$ yields an approximate expression for ζ:

$$\zeta \cong \gamma \, \zeta_{A_0} + (1 - \gamma) \, \zeta_{B_0} \tag{44}$$

where ζ_{A_0} and ζ_{B_0} are the asymptotic success probabilities of the constituent one-mode processes.

The use of this approximation as a means toward gaining an intuitive understanding of the utility of feedback in a two-mode process will be illustrated in the next chapter.

The error involved in the approximation will be illustrated under the Two-Mode Example — Part 2 on page 35.

4. A TWO-MODE EXAMPLE - PART 1

In this chapter we apply the preceding techniques to a study of the effectiveness of simple incremental training in a two-mode TLP. In Chapter 7, we illustrate the use of these techniques in synthesizing a train-work schedule for the two-mode TLP.

In 1960, E. N. Gilbert published a paper describing a Markov model of a two-mode communication channel [ref. 3]. Gilbert called it a burst-noise channel. In this channel, $\underset{\sim}{A}$ and $\underset{\sim}{B}$ of Figure 2 denote the good and bad modes, respectively.

The noise in mode $\underset{\sim}{A}$ is such that by proper choice of a threshold in the observer (or receiver) all transmitted 0's and 1's can be identified without error. The noise in mode $\underset{\sim}{B}$, however, is such that the constituent probability densities of the received signals caused by 0's and 1's overlap, so that error-free detection is impossible, although a proper choice of threshold will minimize the error probability. To simplify our calculations and at the same time preserve qualitative relationships, we assumed that the constituent densities have the staircase shapes shown in Figure 7. Readers familiar with Sklansky's earlier work will recognize each of the modes in Figure 7 as Model I of a quantal TLP [ref. 2]. Hence we refer to the overall system as a two-mode TLP.
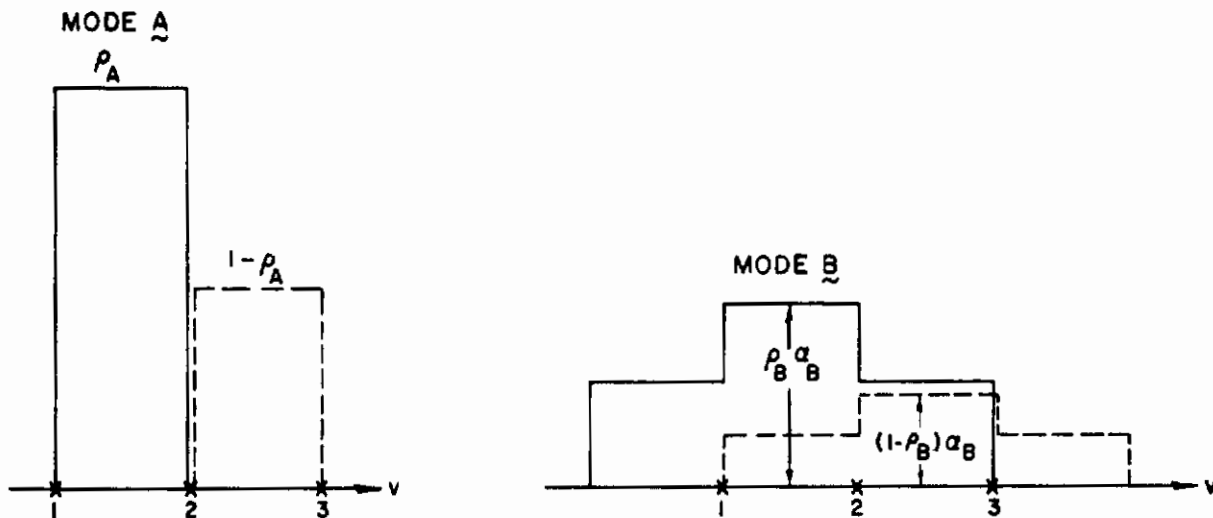
Fig. 7. The Constituent Probability Densities in the Illustrative Example.

The constituent densities of this model have the following properties: (a) the frequencies of occurrence of the transmitted signals in mode $\underset{\sim}{A}$ are equal to the corresponding frequencies in mode $\underset{\sim}{B}$; (b) the variances of the constituent densities in mode $\underset{\sim}{A}$ are fixed, while the variances in $\underset{\sim}{B}$ are variable. Expressed symbolically, these properties are: (a) $\rho_A = \rho_B$; (b) $\alpha_A = 1$. Thus the four constituent densities can be specified by only two parameters: ρ_A (or ρ_B) and α_B. Let

$$\rho \overset{\Delta}{=} \rho_A = \rho_B \tag{45}$$

and

$$\alpha \overset{\Delta}{=} \alpha_B \tag{46}$$

13

Two more parameters complete the specification of the two-mode process: δ and ϵ. In the present example we assumed $\delta << 1$, $\epsilon << 1$. For this case the asymptotic success probability ζ is dependent primarily on the ratio

$$\gamma \overset{\Delta}{=} \frac{\epsilon}{\delta + \epsilon} \tag{47}$$

and only weakly on δ and ϵ individually.

Recapitulating: In the two-mode TLP under analysis, we assume $\delta << 1$, $\epsilon << 1$. For this case the process is completely specified by three parameters: ρ, a, and γ, defined in Equations 45 to 47.

For the specific densities shown in Figure 7, the best performance for mode A is obtained when the threshold is fixed at k =2, and the best threshold for mode B is obtained when the threshold is fixed at k = 3. One will suspect, therefore, that for certain values of a and ρ, no fixed threshold will yield near-optimal performance in the two-mode process, and that continual retraining of the threshold is necessary to obtain near-optimal performance. We shall show that this conjecture is correct over a wide range of ρ, a, and γ.

DERIVATION OF THE TWO-MODE ζ CONTOURS

Equation 44 gives us an easy way to estimate the ζ contours of a weakly coupled two-mode process: First find expressions for the A-only and B-only asymptotic success probabilities, namely ζ_{Ao} and ζ_{Bo}. Then sum these probabilities linearly in accordance with Equation 44. This method of estimating the ζ contours is illustrated below for the two-mode TLP:

$$\underset{\sim}{A} \text{ only:} \quad \zeta_{Ao} = 1 \text{ for all } \rho, a. \tag{48}$$

$$\underset{\sim}{B} \text{ only:} \quad \zeta_{Bo} = \frac{a + Q}{1 + Q} \tag{49}$$

$$\text{where} \quad Q \overset{\Delta}{=} \frac{1 - a}{1 + a} \frac{1 - \rho}{\rho} + \frac{\rho}{1 - \rho}. \tag{50}$$

$$\text{Two-mode:} \quad \zeta \cong \gamma \zeta_{Ao} + (1 - \gamma) \zeta_{Bo} \tag{51}$$

$$= \gamma + (1 - \gamma) \frac{a + Q}{1 + Q} \tag{52}$$

where Q is given by Equation 50.

An alternative formula for ζ is

$$\zeta = \gamma + (1 - \gamma) \zeta_{Bo} \tag{53}$$

where ζ_{Bo} is given by Equation 49.

Thus the ζ contours may be estimated merely by relabeling the ζ_{Bo} contours. The latter contours, which appeared in an earlier report [ref. 2], are reproduced here in Figure 8.

14
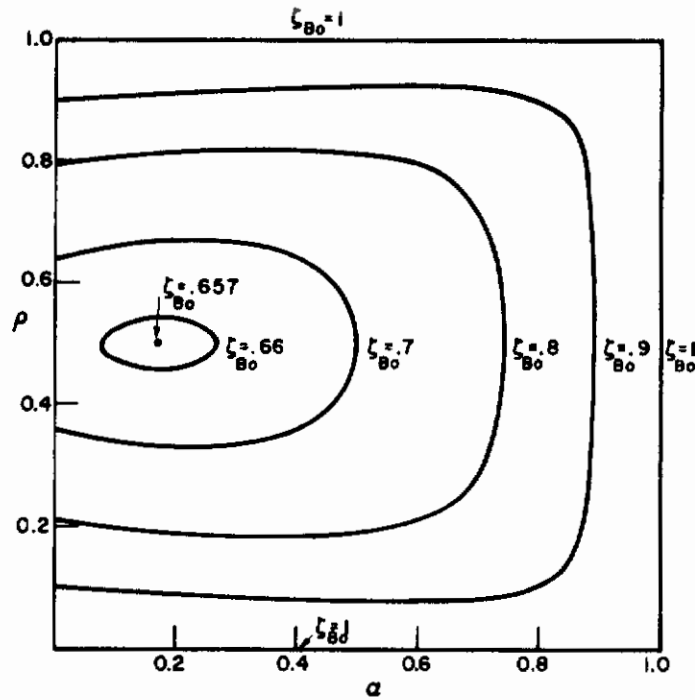
Figure 8. ζ_{Bo} Contours.

For convenience, we shall assume hereafter that $y = \frac{1}{2}$. For this case Equation 53 becomes

$$\zeta = \frac{1}{2} (1 + \zeta_{Bo}) \tag{54}$$

Using this equation the ζ_{Bo} contours of Figure 8 are easily relabeled to form the ζ contours of the two-mode process. The resulting contours are shown as the unbroken curves in Figure 9.
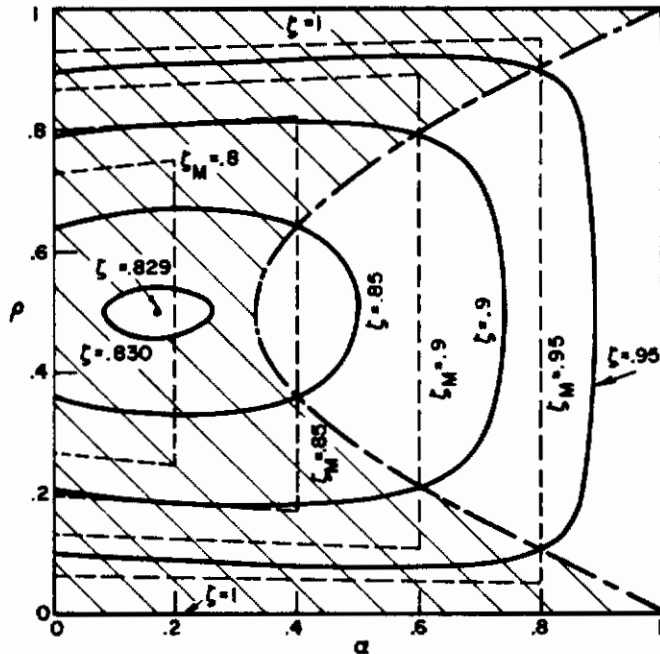
Figure 9.   The Unbroken Curves Show the Two-Mode ζ Contours for $y = \frac{1}{2}$.

15

THE BEST-FIXED-THRESHOLD PERFORMANCE

We know that in one-mode TLPs a fixed-threshold operation can yield success probabilities that are greater than those obtained from simple incremental training, provided that the fixed threshold is properly chosen. In fact for a properly chosen threshold in a one-mode TLP, the resulting success probabilities cannot be exceeded by any other threshold control policy.

In two-mode TLPs, on the other hand, the best possible fixed-threshold policy can often be outperformed by a simple incremental feedback policy. To demonstrate this fact and to determine the region of parameter space in which incremental feedback outperforms the best-fixed-threshold policy, we computed the success probability contours resulting from a best-fixed-threshold policy. We denote them as the ζ_M-contours. The derivation of these contours is summarized below.

$\underset{\sim}{A}$ only:

$$\zeta_{Ao1} = 1 - \rho \tag{55}$$

$$\zeta_{Ao2} = 1 \tag{56}$$

$$\zeta_{Ao3} = \rho \tag{57}$$

(The subscripts following Ao indicate the value of the fixed threshold. For example, ζ_{Ao2} is the success probability in mode $\underset{\sim}{A}$ when k = 2.)

$\underset{\sim}{B}$ only:

$$\zeta_{Bo1} = 1 - \frac{\rho}{2} (1 + a) \tag{58}$$

$$\zeta_{Bo2} = \frac{1 + a}{2} \tag{59}$$

$$\zeta_{Bo3} = 1 - \frac{1 - \rho}{2} (1 + a). \tag{60}$$

Two-mode:

When the threshold of a two-mode process is fixed, the process is described exactly by a two-state Markov chain of the form shown in Figure 2, where the square nodes are to be interpreted as ordinary states. For this chain, the asymptotic probabilities of states $\underset{\sim}{A}$ and $\underset{\sim}{B}$ are γ and $1 - \gamma$, respectively. Hence, the success probability of this process is exactly

$$\zeta_k = \gamma \zeta_{Aok} + (1 - \gamma) \zeta_{Bok} \tag{61}$$

Substituting Equations 55 to 60 in Equation 61 yields the following formulas for the two-mode fixed-threshold asymptotic success probabilities:

$$\zeta_1 = 1 - \rho \gamma - (1 - \gamma) \rho \frac{1 + a}{2} \tag{62}$$

$$\zeta_2 = \gamma + (1 - \gamma) \frac{1 + a}{2} \tag{63}$$

$$\zeta_3 = 1 - \gamma (1 - \rho) - (1 - \gamma)(1 - \rho) \frac{1 + a}{2} \tag{64}$$

16

When $y = \frac{1}{2}$, these formulas become

$$\zeta_1 = 1 - \frac{\rho}{4}(3 + a) \tag{65}$$

$$\zeta_2 = \frac{3 + a}{4} \tag{66}$$

$$\zeta_3 = 1 - (1-\rho)\frac{3 + a}{4} \tag{67}$$

Equations 65 to 67 may be rewritten in the following form:

$$\rho = \frac{4(1 - \zeta_1)}{3 + a} \tag{68}$$

$$a = 4\zeta_2 - 3 \tag{69}$$

$$1 - \rho = \frac{4(1 - \zeta_3)}{3 + a} \tag{70}$$

These equations are in a convenient form for plotting the ζ_k contours. The resulting ζ_k maps are given in Figures 10, 11, and 12.

The best-fixed-threshold asymptotic performance is

$$\zeta_M = \underset{k}{\text{Max}} \ \zeta_k \tag{71}$$

The ζ_M contours were obtained graphically by superposing the maps of $\zeta_1, \zeta_2,$ and ζ_3. The resulting ζ_M contours are shown in Figure 13. These contours describe the asymptotic performance of the best-fixed-threshold process.
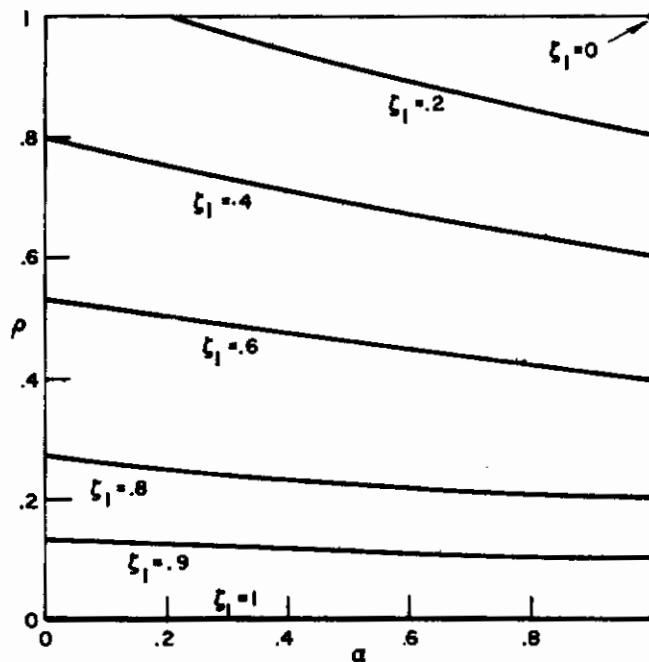

Figure 10. ζ_1 Contours for $y = \frac{1}{2}$.

17
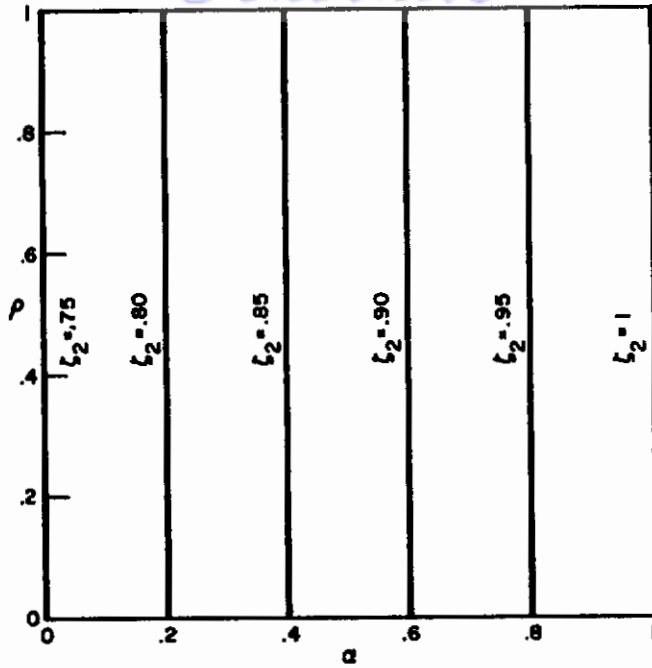
Figure 11. ζ_2 Contours for $\gamma = \dfrac{1}{2}$.

Figure 12. ζ_3 Contours for $\gamma = \dfrac{1}{2}$.

18
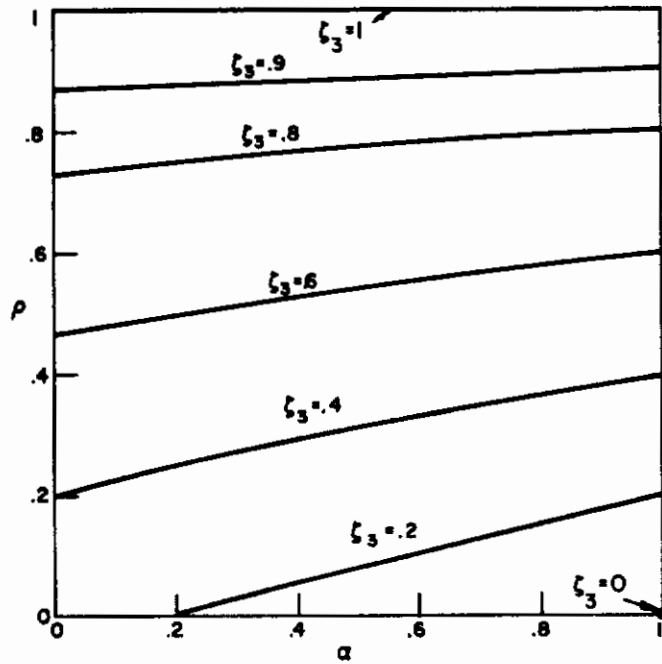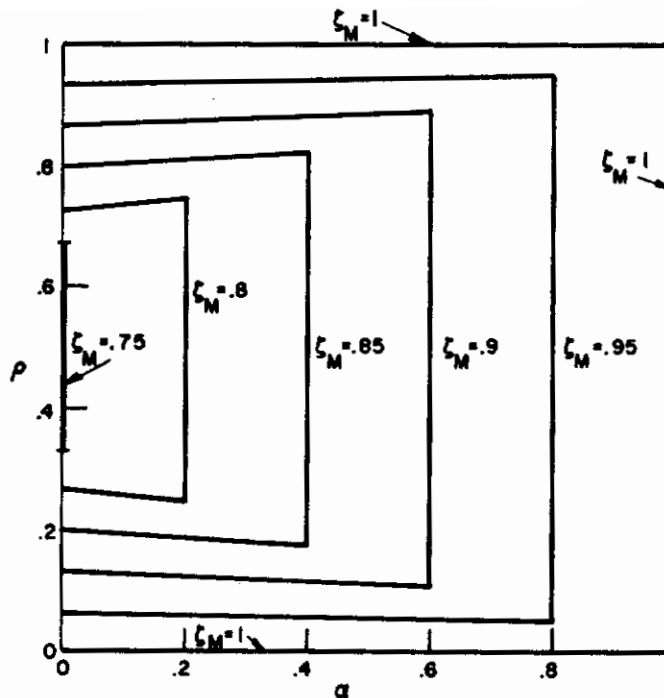
Figure 13. ζ_M Contours for $\gamma = \frac{1}{2}$.

DISCUSSION OF THE ζ AND ζ_M CONTOURS

The assumption $\delta \ll 1$, $\epsilon \ll 1$ greatly facilitates the construction of the ζ contours, since under this assumption ζ is a linear combination of ζ_{Ao} and ζ_{Bo}. The ζ_M contours, on the other hand, are always easy to construct, because ζ_k is a linear combination of ζ_{Aok} and ζ_{Bok} for all values of δ and ϵ. No approximation is involved in Equation 61.

If we compare the ζ contours and the ζ_{Bo} contours, we see how the good mode expands the acceptable stability-reliability zone. In particular, if we define the acceptable zone as the region of the $a\rho$-square for which $\zeta \geq 0.9$, we see that the acceptable zone of the ζ map is about twice as large as that of the ζ_{Bo} map.

To facilitate a comparison between the ζ maps and the ζ_M maps, we have plotted the ζ_M contours as dashed lines in Figure 9. We see that $\zeta > \zeta_M$ over a large region of the $a\rho$-square. This observation confirms our conjecture that for some values of a and ρ a simple incremental feedback policy will yield better asymptotic performance than any fixed-threshold policy. This region, which is shaded in Figure 9, is bounded on the right by the dash-dotted line. This dash-dotted line remains fixed for all γ in the range $\gamma_o \leq \gamma < 1$, where $\gamma_o \cong \frac{1}{3}$. (The value of γ_o was computed from data taken from Figure 9.)

Consequently, if we know a priori that (a, ρ) lies within the unshaded region of Figure 9, then a fixed threshold, fixed at $k = 2$, will yield better performance than a process trained by a simple incremental feedback policy. On the other hand, since the shaded region of Figure 9 occupies an area significantly greater than half of the $a\rho$-square, a simple incremental policy will on the average yield better performance than any fixed-threshold policy, if we assume that all pairs (a, ρ) are equally likely. If $a < \frac{1}{3}$ is not admissible (which is the case if no two-peak

19

constituent densities are admissible) then the shaded region occupies slightly less than one-half of the admissible area of the $a\rho$-square. Hence if $a < \frac{1}{3}$ is not admissible, a simple incremental policy will on the average yield slightly worse performance than the best-fixed-threshold policy, if all pairs (a, ρ) in the region $\frac{1}{3} \leq a \leq 1, 0 \leq \rho \leq 1$ are equally likely.

An interesting extension of the present work would be an investigation of the effect of raising the number of thresholds on the size of the region over which $\zeta > \zeta_M$. We believe that when the distance between the constituent modes' optimum thresholds is greater than in the present example, then the shaded area will occupy a greater fraction of the parameter space.

THE ULTIMATE ASYMPTOTIC PERFORMANCE

One can conceive of a threshold adjustment that would yield the ultimate in success probability. It would be as follows: Whenever the process shifts to mode $\underset{\sim}{A}$, the threshold immediately shifts to the best $\underset{\sim}{A}$-only threshold. The threshold remains at the best $\underset{\sim}{A}$-only threshold as long as the process remains in mode $\underset{\sim}{A}$. When the process shifts to mode $\underset{\sim}{B}$, the threshold immediately shifts to the best $\underset{\sim}{B}$-only threshold, and stays there as long as the process remains in $\underset{\sim}{B}$. No better performance can be obtained, since the threshold is perfectly matched to the mode at every instant. The asymptotic success probability of this feedback policy is:

$$\zeta_U = \gamma \zeta_{AoM} + (1 - \gamma) \zeta_{BoM} \tag{72}$$

since the process spends the fraction γ of its time in mode $\underset{\sim}{A}$ and $1 - \gamma$ in mode $\underset{\sim}{B}$. (U stands for "ultimate.") Since the ζ_M contours of one-mode TLPs are obtainable from the ζ_k contours, the ζ_U contours are also obtainable from the ζ_k contours. Thus:

$$\zeta_U = \gamma \underset{k}{\text{Max}} (\zeta_{Aok}) + (1 - \gamma) \underset{k}{\text{Max}} (\zeta_{Bok}). \tag{73}$$

Consequently the ζ_U contours of the two-mode TLP are easily found from the fixed-threshold performance contours of the constituent one-mode TLPs.

A natural question is: How closely do the ζ contours approach the ζ_U contours? In our two-mode example, $\zeta_{AoM} = 1$ and $\gamma = \frac{1}{2}$. For this case, Equation 72 becomes

$$\zeta_U = \frac{1}{2} (1 + \zeta_{BoM}) \tag{74}$$

With the aim of answering the above question, the ζ_U contours were plotted as the unbroken curves in Figure 14, and the ζ contours, based on Equation 54, were superimposed as dashed lines in the same figure. (The ζ contours are the same as those in Figure 9.)

If we compare Equation 74 to Equation 54, we note that Figure 14 is identical, except for a labeling of contours, to the superposed ζ_{BoM} and ζ_{Bo} contours, shown in Figure 15. (The latter figure appeared in an earlier report as the ζ_M map for Model I [ref. 2].)

The ζ_U contours are the ultimate performance contours for the two-mode TLP. Actually, no practical feedback policy can ever realize the ζ_U contours, because no finite amount of hardware
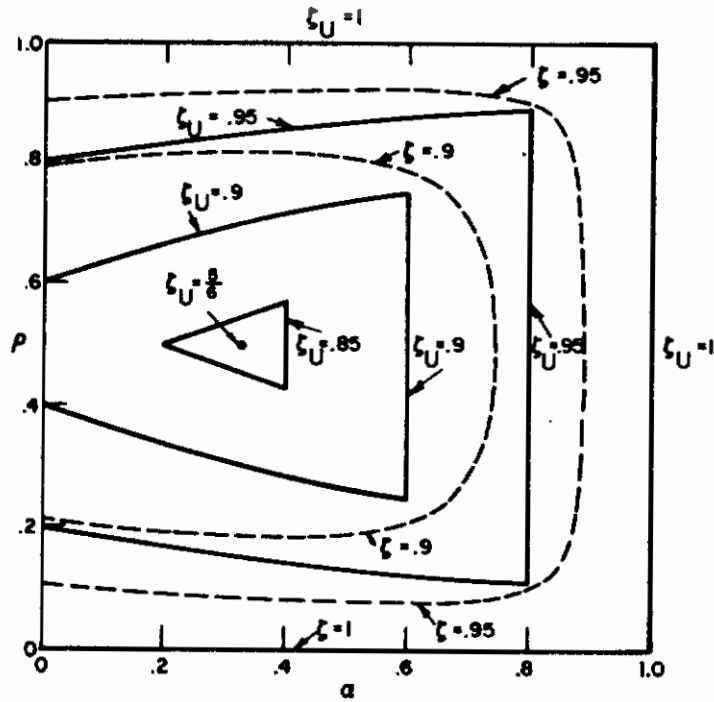
Figure 14. ζ Contours Superposed on ζ_U Contours.

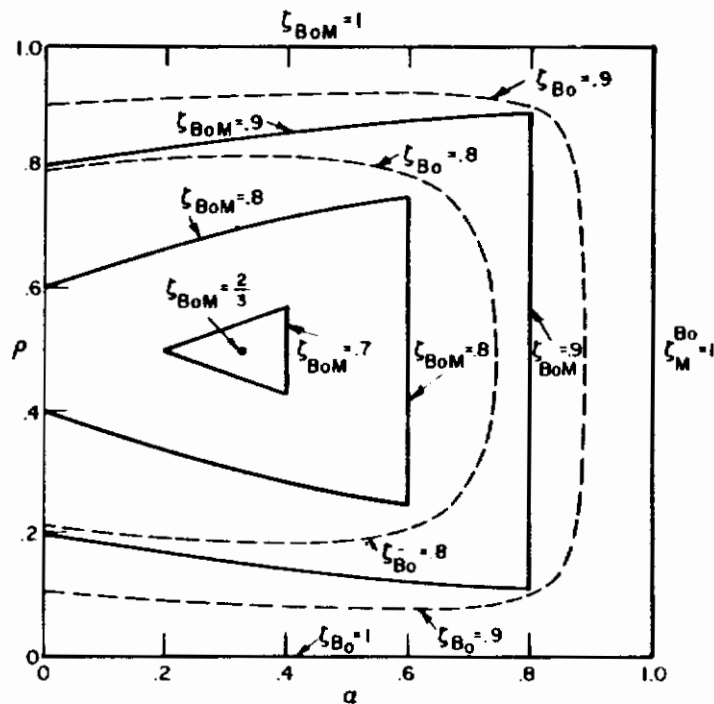Figure 15. ζ_{Bo} Contours Superposed on ζ_{BoM} Contours.

can recognize a sudden change of mode. There will always be a nonzero probability that a change of mode will go unrecognized after a finite time of operation within that mode. Thus the ζ_U contours represent an upper bound on the realizable contours. Is it a *least* upper bound? We suspect so, but have not been able to prove it.

21

Since Figure 14 is obtainable merely by relabeling Figure 15, we see that the ζ contours differ from the ζ_U contours in the same manner as the ζ_{B_0} contours differ from the ζ_{B_0M} contours. Hence, to bring the ζ contours of the two-mode process closer to the ζ_U contours, we may use the same change in feedback policy as would be used in bringing the ζ_{B_0} contours closer to the ζ_{B_0M} contours.

On the other hand, an important difference between Figures 14 and 15 is that the differences between adjacent contours in Figure 14 are one-half of those in Figure 15: in this sense the two-mode ζ's are closer to the ultimate values than the bad-mode ζ's. The reason for this is that in the two-mode process the good mode masks some of the bad mode's misbehavior.

In this connection we also note that the ζ_U contours can serve as a coarse approximation of the ζ contours in the two-mode process, just as the ζ_{B_0M} contours serve as a coarse approximation of the ζ_{B_0} contours [ref. 2]. Thus:

$$\zeta \cong \zeta_U \tag{75}$$

where ζ_U may be computed by Equation 73.

EFFECTIVENESS OF THE FEEDBACK POLICY

We shall show that the effectiveness of simple incremental training in a weakly coupled two-mode TLP is greater than in either of the constituent one-mode processes, where effectiveness is measured as an increase in the stability-reliability area in the $a\rho$-square.

Let $\overline{I}_{A_0}$ denote the average increment in the "good" region of the $a\rho$-square for the $\underset{\sim}{A}$-only process yielded by closing the feedback loop, where the good region is defined as that region where $\zeta \geq 0.8$. (See discussion in ref. 2.) Let $\overline{I}_{B_0}$ and $\overline{I}$ be defined similarly for the $\underset{\sim}{B}$-only process and the two-mode process, respectively.

The value of $\overline{I}_{B_0}$ is available from Table 2 in ref. 2. The value of $\overline{I}$ may be computed by graphical techniques in Figures 9 to 12. The value of $\overline{I}_{A_0}$ is computed as follows:

$$\overline{I}_{A_0} = 1 - \frac{1}{3}(0.2 + 1 + 0.2) = 0.534$$

The results are summarized as follows:

$$\overline{I}_{A_0} = 0.530$$

$$\overline{I}_{B_0} = 0.230$$

$$\overline{I} = 0.583$$

Thus $\overline{I}$ is larger than either $\overline{I}_{A_0}$ or $\overline{I}_{B_0}$. Therefore the effectiveness, in the asymptotic sense, of the simple incremental feedback policy is greater for the two-mode process than for either of the constituent one-mode processes.

When the success probability z(n) is brought to a specified acceptable value, or higher, by the training, the training may be stopped. The process then begins its working phase (i.e., open-loop operation). If the process is a one-mode TLP, z(n) will remain, throughout the working phase, at the value it attained at the end of the training phase. But suppose the process is a two-mode TLP. There exists a nonzero probability of a mismatch between the threshold and the mode, i.e., there is a nonzero probability that the threshold of the process is not optimum for the particular mode the process happens to occupy. In a two-mode process, this mismatch probability is relatively small at the end of the training phase, and becomes greater and greater as the process moves further along in the working phase. (In a one-mode process, the mismatch probability remains constant throughout the working phase.) Hence one expects the success probability during the working phase of a two-mode process to diminish monotonically from a peak at the beginning of the working phase, finally leveling off at an asymptotic value ζ_F. (The subscript F stands for "fixed threshold".) We shall show how the Markov chain model permits an exact analysis of the dynamics of the working-phase success probability. It also permits a determination of ζ_F.

Suppose we want the success probability to remain above a prescribed lower bound ζ_L, throughout the working phase. If $\zeta_L > \zeta_F$, then the working phase will have to be interleaved with retraining phases. We shall show how the Markov chain model permits us to find an optimum train-work schedule for any specific ζ_L. Simplified techniques for approximate estimates of the train-work dynamics will also be presented. These techniques will be illustrated under the Two-Mode Example − Part 2 on page 35.

DERIVATION OF THE WORKING-PHASE PERFORMANCE WAVE

The basic formula for the working-phase success probability $z_F(n)$ is:

$$z_F(n) = \underline{r}(n) \, \underline{q} \tag{76}$$

$$\equiv \left[\underline{r}_A(n), \, \underline{r}_B(n) \right] \left[\underline{q}_A, \, \underline{q}_B \right] \tag{77}$$

where $r_{Ak}(n)$ is the joint probability that the process will occupy mode $\underset{\sim}{A}$ and threshold k at time n, q_{Ak} is the probability of success when the process occupies mode $\underset{\sim}{A}$ and threshold k, and n = 0 is the final instant of the training phase. Equation 77 will help us find an expression for $z_F(n)$ in terms of the state probabilities at time n = 0 and certain open-loop transition probabilities.

For any particular threshold k, the working-phase signal flow graph will be that of Figure 16. This graph yields the following expressions for the x-transforms of the state probabilities:
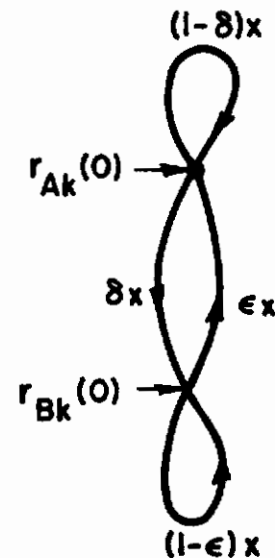

Figure 16. A Working-Phase Signal Flow Graph.

23

$$\underset{\sim}{r}_{Ak}(x) = \frac{1}{D(x)} \left\{ r_{Ak}(0) [1 - (1-\epsilon)x] + r_{Bk}(0) \epsilon x \right\} \tag{78}$$

$$\underset{\sim}{r}_{Bk}(x) = \frac{1}{D(x)} \left\{ r_{Bk}(0) [1 - (1-\delta)x] + r_{Ak}(0) \delta x \right\} \tag{79}$$

where

$$D(x) \overset{\Delta}{=} (1 - x) [1 - (1 - \delta - \epsilon) x] \tag{80}$$

We shall assume that the mode-to-mode transitions began at $n = -\infty$, so that the elements of $\underline{r}_A(n)$ and of $\underline{r}_B(n)$ at $n \geq 0$ sum to γ and $1 - \gamma$, respectively. It is therefore convenient to define the two normalized vectors $\hat{\underline{r}}_A(n)$ and $\hat{\underline{r}}_B(n)$, obtained by dividing $\underline{r}_A(n)$ and $\underline{r}_B(n)$ by γ and $1 - \gamma$, respectively. (We may think of $\hat{\underline{r}}_A(n)$ as a conditional probability vector, given that the process occupies mode $\underset{\sim}{A}$.) Thus we have

$$\left. \begin{aligned} \underline{r}_A(n) &\overset{\Delta}{=} \gamma \, \hat{\underline{r}}_A(n) \\[2mm] \underline{r}_B(n) &\overset{\Delta}{=} (1 - \gamma) \, \hat{\underline{r}}_B(n) \end{aligned} \right\} \tag{81}$$

Substituting Equations 78 to 80 in the x-transform of Equation 77, and making use of Equations 81 and 20, we obtain the following expression for the x-transform of the working-phase success probability:

$$\underset{\sim}{z}_F(x) = \frac{1}{(\delta + \epsilon) D(x)} \left\{ \epsilon \psi_A [1 - (1 - \epsilon)x] + \delta \psi_B [1 - (1 - \delta)x] + \delta \epsilon (\psi_{AB} + \psi_{BA}) x \right\} \tag{82}$$

where

$$\left. \begin{aligned} \psi_A &\overset{\Delta}{=} \hat{\underline{r}}_A(0) \, \underline{q}_A \\[2mm] \psi_B &\overset{\Delta}{=} \hat{\underline{r}}_B(0) \, \underline{q}_B \\[2mm] \psi_{AB} &\overset{\Delta}{=} \hat{\underline{r}}_A(0) \, \underline{q}_B \\[2mm] \psi_{BA} &\overset{\Delta}{=} \hat{\underline{r}}_B(0) \, \underline{q}_A \end{aligned} \right\} \tag{83}$$

and where $D(x)$ is given by Equation 80. Recall that $\underline{q}_A$ and $\underline{q}_B$ are column vectors, so that the products in Equations 83 are inner products.

A convenient expression for the asymptotic working-phase success probability, ζ_F, is obtainable with the aid of the "final-value theorem" for x-transforms [ref. 6]:

$$\zeta_F \overset{\Delta}{=} \lim_{n \to \infty} z_F(n) = \lim_{x \to 1} [(1 - x) \, z_F(x)] \tag{84}$$

Substituting Equation 80 in Equation 82, and applying Equation 84 to the resulting expression, yields

$$\zeta_F = \gamma^2 \psi_A + (1 - \gamma)^2 \psi_B + \gamma(1 - \gamma)(\psi_{AB} + \psi_{BA}). \tag{85}$$

24

A formula for the value of $z_F(n)$ at the beginning of the work cycle is obtainable from the zero-order term of the power-series expansion of Equation 82:

$$z_F(0) = \underset{\sim}{z}_F(0) = \gamma \psi_A + (1-\gamma) \psi_B \qquad (86)$$

This checks the fact that $z_F(0)$ equals the last value of $z(n)$ in the training phase.

The following question arises: Under what conditions will the distance between $z_F(0)$ and ζ_F be maximized? A comparison of Equations 85 and 86 shows that this distance is maximized when $\psi_{AB} = \psi_{BA} = 0$, assuming γ, ψ_A, and ψ_B are fixed. Note in Equation 83 that ψ_{AB} and ψ_{BA} are "cross-correlations" between the conditional success vectors of one mode and the threshold vectors of the other mode. This distance is maximized further if we set $\gamma = 1/2$. Under this condition, $z_F(0) = 2 \zeta_F$. Thus: *the final success probability in a working phase of any two-mode process cannot be less than one-half of the success probability at the beginning of that working phase.*

Because $D(x)$ can be factored into the two linear portions shown in Equation 80, $\underset{\sim}{z}_F(x)$ can be expressed in the following partial-fraction form:

$$\underset{\sim}{z}_F(x) = \frac{P}{1-x} + \frac{Q}{1-(1-\delta-\epsilon)x} \qquad (87)$$

By Equations 84, 86, and 87, we find that $P = \zeta_F$ and $Q = z_F(0) - \zeta_F$. Hence

$$z_F(n) = \zeta_F + \left[z_F(0) - \zeta_F \right] (1-\delta-\epsilon)^n \qquad (88)$$

where $z_F(0)$ and ζ_F are given by Equations 86 and 85. Note that Equation 88 is exact — no approximations are involved.

Equation 88 displays the degradation in performance associated with the working phase. That this degradation is brought about by the mode-to-mode fluctuations is displayed by the fact that the exponentially decaying portion of Equation 88 decays at a rate determined only by δ and ϵ. Another factor involved in determining the extent of the working-phase degradation is the degree of mismatch that occurs when a threshold optimized for one mode coexists with the other mode. This is seen when we compare Equations 85 and 88, and take note of the definitions in Equation 83. If modes $\underset{\sim}{A}$ and $\underset{\sim}{B}$ were identical, then ζ_F would equal $z_F(0)$. As we have seen, the degree to which ζ_F and $z_F(0)$ differ depends on the sizes of ψ_{AB} and ψ_{BA}.

Note also that $z_F(n)$ is not sensitive to changes in the initial threshold probability vector, $\underline{r}_A(0)$ and $\underline{r}_B(0)$, provided $z_F(0)$ and ζ_F are fixed. Thus $z_F(0)$ and ζ_F completely determine the working phase performance, and no knowledge of the individual initial threshold probabilities is required.

6. TRAIN-WORK CYCLES

We have seen that the mode-to-mode fluctuations of a two-mode process effect a degradation of performance during a working phase. A schedule of train, work, retrain, work, retrain, etc., will therefore be necessary if the lowest acceptable success probability is greater than ζ_F.

This is to be contrasted to one-mode processes, where a single training phase can bring the success probability permanently to a desired value. No retraining is needed because no degradation of performance takes place in a working phase of a one-mode process. We have seen that the two-mode closed-loop performance (success probability during a training phase) is only weakly dependent on δ and ϵ when δ and ϵ are small. The closed-loop two-mode performance for small δ and ϵ is approximately equal to a weighted sum of the $\underset{\sim}{A}$-only and $\underset{\sim}{B}$-only closed-loop performances. On the other hand, the two-mode, open-loop performance (success probability during a working phase) is, as we have seen, strongly dependent on δ and ϵ, even when δ and ϵ are small.

We shall show how train-work schedules may be constructed from a knowledge of the $\underset{\sim}{A}$-only and $\underset{\sim}{B}$-only behaviors. We shall also show how increased accuracy in the design of a train-work schedule may be obtained from a knowledge of the exact two-mode performance during a single training phase.

EXACT ANALYSIS

An exaggerated example of a train-work cycle is illustrated in Figure 17. During the training
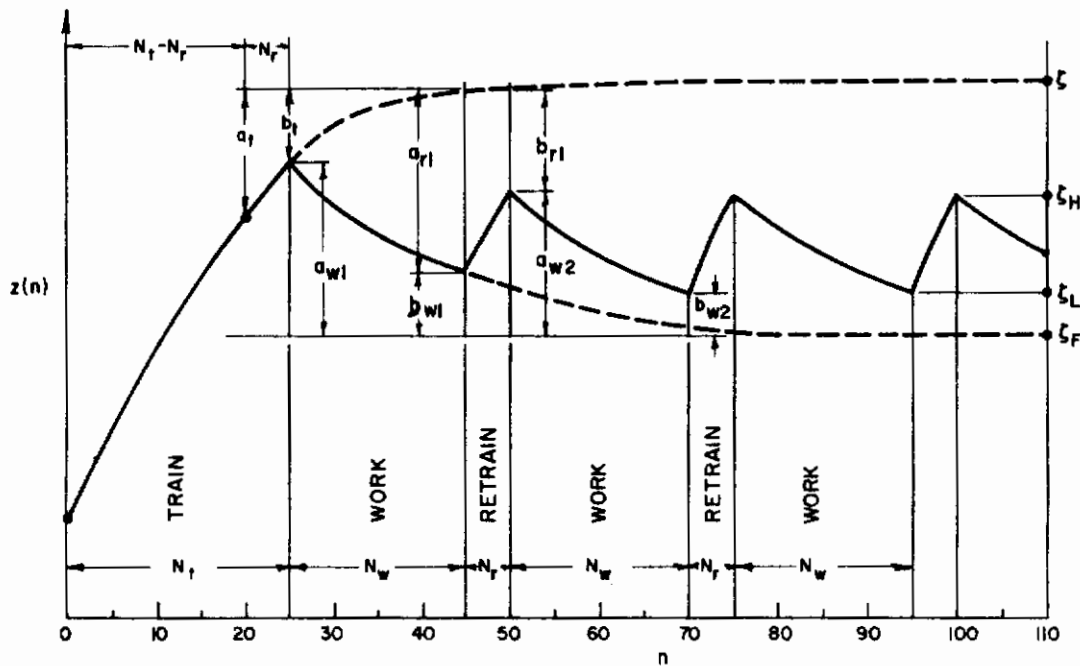

Figure 17. A Train-Work Cycle.

phase, the threshold probability vector is

$$\underline{r}(n) = \underline{r}(0) \ (\underline{\Gamma} \ \underline{P})^n \tag{89}$$

26

where

$$\underline{r}(0) = \left[\underline{r}_A(n), \underline{r}_B(n)\right]$$

$$\underline{\Gamma} = \begin{bmatrix} 1-\delta & \delta \\ \epsilon & 1-\epsilon \end{bmatrix}$$

$$\underline{P} = \begin{bmatrix} \underline{A} & \underline{0} \\ \underline{0} & \underline{B} \end{bmatrix}$$

$$\underline{0} \overset{\Delta}{=} \text{ a square matrix every element of which is zero.}$$

For example, if the process involves three thresholds (k = 1, 2, 3), if the initial threshold is k = 1, if $\gamma = 1/2$, and if the mode-to-mode fluctuations started at $n = -\infty$, then

$$\underline{r}_A(0) = \underline{r}_B(0) = \left(\frac{1}{2}, 0, 0\right)$$

and

$$\underline{r}(0) = \left(\frac{1}{2}, 0, 0, \frac{1}{2}, 0, 0\right).$$

The training performance wave is given by

$$z(n) = \left[\underline{r}_A(n), \underline{r}_B(n)\right]\left[\underline{q}_A, \underline{q}_B\right].$$

Expressions for $\underline{q}_A$ and $\underline{q}_B$ in terms of the constituent one-mode conditional success vectors are given by Equation 37.

Suppose the training phase lasts until $n = N_t$. The threshold vector at $n = N_t$ is

$$\underline{r}(N_t) = \underline{r}(0) \, (\underline{\Gamma} \, \underline{P})^{N_t}$$

$$= \left[r_{A1}(N_t), \, r_{A2}(N_t), \, r_{A3}(N_t), \, r_{B1}(N_t), \, r_{B2}(N_t), \, r_{B3}(N_t)\right]$$

The meaning of this vector is made clear by the following definition:

$$r_{A1}(N_t) = \text{joint probability of mode } \underset{\sim}{A} \text{ and threshold 1}$$
$$\text{at } n = N_t.$$

Immediately following $n = N_t$, the first working phase begins, and lasts until $n = N_t + N_w$. During the working phase, the threshold probability vector is

$$\underline{r}(N_t + m) = \left[\underline{r}_1(N_t + m), \, \underline{r}_2(N_t + m), \, \underline{r}_3(N_t + m)\right]$$

where

$$\underline{r}_k(N_t + m) \overset{\Delta}{=} \left[r_{Ak}(N_t + m), \, r_{Bk}(N_t + m)\right]$$

27

This means that during the working phase, the threshold is fixed at a specific value, but the choice of this value is determined by the joint probability distributions $r_{Ak}(n)$ and $r_{Bk}(n)$. For any specific threshold k, the two-dimensional vector $\underline{r}_k(N_t + m)$ is transformed by the two-mode open-loop Markov chain of Figure 16. The total working-phase threshold probability vector is just the union of $\underline{r}_k(N_t + m)$ over k.

The working phase threshold probability as a function of m is found either from Equations 78 and 79 or from the following equation:

$$\underline{r}_k(N_t + m) = \left[r_{Ak}(N_t), \; r_{Bk}(N_t) \right] \begin{bmatrix} 1-\delta & \delta \\ \epsilon & 1-\epsilon \end{bmatrix}^n \tag{90}$$

for $m = 1, 2, \ldots, N_w$.

The success probability during this working phase is found from Equation 88. Alternatively, we may find it as follows:

$$z_{Fk}(N_t + m) \overset{\Delta}{=} \underline{r}_k(N_t + m) \, \underline{q}_k$$

where

$$\underline{q}_k \overset{\Delta}{=} (q_{Ak}, q_{Bk})$$

Then,

$$z_F(N_t + m) = \sum_k z_{Fk}(N_t + m)$$

$$= \sum_k \left[\underline{r}_k(N_t + m) \, \underline{q}_k \right]$$

for $m = 1, 2, \ldots, N_w$.

The retraining phase starts at $n = N_t + N_w$ and lasts until $n = N_t + N_w + N_r$. The threshold probability vector during this phase is found by replacing $\underline{r}(0)$ in Equation 89 by $\underline{r}(N_t + N_w)$ and by an appropriate adjustment of the exponent:

$$\underline{r}(N_t + N_w + m) = \underline{r}(N_t + N_w) \, (\underline{\Gamma} \, \underline{P})^m \tag{91}$$

Recapitulating: Suppose the available thresholds range over the values $k = 1, 2, \ldots, K$. At the end of the training phase, the 2K elements of the threshold probability vector $\underline{r}(N_t)$ are grouped into pairs — each pair consisting of the two joint probabilities associated with the same threshold k. These pairs are then used in Equation 90 to find the corresponding pairs throughout the working phase. At the end of the working phase the pairs are regrouped into a 2K-dimensional vector, $\underline{r}(N_t + N_w)$. This new vector is used as the initial condition for the retraining phase, and used in Equation 91 to find the threshold probability throughout the retraining phase.

A significant computational difficulty in the exact analysis of the two-mode process is the task of regrouping $\underline{r}(n)$ at the transition between training and working phases. We believe, however, that these transition regroupings may be ignored in many cases without incurring serious errors.

28

An analysis technique based on ignoring the transition regroupings is described in the next section This technique will be illustrated under Two-Mode Example — Part 2 on page 35.

THE RC-CIRCUIT APPROXIMATION

We shall now describe a convenient approximate method for analyzing train-work cycles. The method is based on the assumption that when the training performance wave $z(n)$ is near its asymptote, $z(n)$ may be approximated by the sum of a constant term and only one exponentially decaying term — i.e., only one nonconstant eigenfunction. (Actually, $z(n)$ contains five nonconstant eigenfunctions.) This assumption automatically implies that the transition regroupings may be ignored, since a change in the transition regroupings only affects the degree to which each eigenfunction contributes to $z(n)$. The value of ζ is unaffected by the transition regroupings, because the nth power of any ergodic stochastic matrix approaches a limit that is independent of the initial matrix. Another property implied by the assumption of only one nonconstant eigenfunction in the training performance waves is that the ζ_F's of all the working phases are identical. Actually, the ζ_F of any working phase is dependent on the specific distribution of threshold probabilities at the beginning of that phase.

Another assumption of the approximation to be described is that the one-mode threshold-probability waves are either known or are computable without undue strain. These one-mode threshold-probability functions are basic elements in our analysis method.

The form of the train-work cycle that we shall analyze is illustrated in Figure 17. This cycle consists of three types of phases: (1) a training phase, (2) a working phase, and (3) a retraining phase. The first phase is a training phase, lasting for N_t time units. The second phase is a working phase, lasting for N_w time units. This is followed by a retraining phase, lasting for N_r time units, after which, the working and retraining phases are repeated indefinitely, the phase durations remaining at N_w and N_r, respectively. In Figure 17, the oscillations are exaggerated for clarity of illustration. In real situations the oscillations will be much smaller.

The train-work cycle of Figure 17 is analogous to the charge-discharge cycle of a resistor-capacitor circuit, such as that illustrated in Figure 18. Consequently we refer to this approximation technique as the RC-circuit approximation.
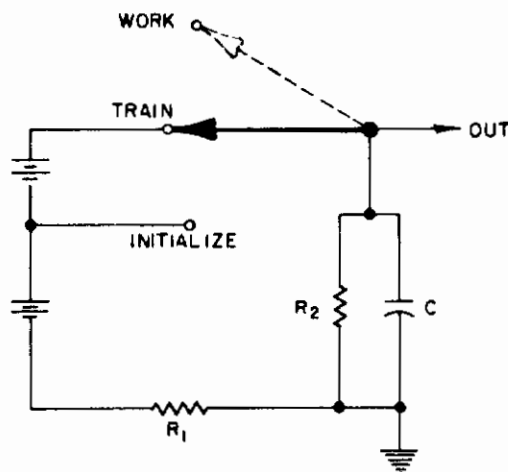

Figure 18. An Approximate Electrical Analog of the Train-Work Cycle.

Because the training phase is assumed to have only one nonconstant eigenfunction, the ratios b_t/a_t, b_{r1}/a_{r1}, etc. in Figure 17 are all equal. Call this ratio θ_r. We have shown that the working phase performance wave contains exactly one nonconstant eigenfunction (Equation 88). Hence the ratios b_{w1}/a_{w1}, b_{w2}/a_{w2}, etc. in Figure 17 are all equal. Call this ratio θ_w.

Because $b_{ri}/a_{ri} = \theta_r$ and $b_{wi}/a_{wi} = \theta_w$ for all i, the asymptotic lower bound ζ_L and the asymptotic upper bound ζ_H (H stands for "high") may be expressed as the following functions of θ_r, θ_w, ζ, and ζ_F:

$$\zeta_L = \zeta_F + (\zeta - \zeta_F) \frac{(1 - \theta_r)\,\theta_w}{1 - \theta_r\,\theta_w} \tag{92}$$

$$\zeta_H = \zeta_F + (\zeta - \zeta_F) \frac{1 - \theta_r}{1 - \theta_r\,\theta_w} \tag{93}$$

The derivation of these formulas is easy, making use of the sums of geometric series, and is omitted.

Equations 92 and 93 may be simplified if we normalize ζ_L and ζ_H with respect to ζ and ζ_F as follows:

$$\hat{\zeta}_L \overset{\Delta}{=} \frac{\zeta_L - \zeta_F}{\zeta - \zeta_F} \tag{94}$$

$$\hat{\zeta}_H \overset{\Delta}{=} \frac{\zeta_H - \zeta_F}{\zeta - \zeta_F} \tag{95}$$

Using these definitions, Equations 92 and 93 become

$$\hat{\zeta}_L = \frac{(1 - \theta_r)\,\theta_w}{1 - \theta_r\,\theta_w} \tag{96}$$

$$\hat{\zeta}_H = \frac{1 - \theta_r}{1 - \theta_r\,\theta_w} \tag{97}$$

Note that

$$\hat{\zeta}_L = \hat{\zeta}_H\,\theta_w \tag{98}$$

We yet have to show how to estimate θ_r and θ_w. The value of θ_r may be estimated from the nonconstant eigenfunctions of the constituent one-mode processes. (The way this is done will be shown in the numerical example of the next chapter.) The value of θ_w is easy to find:

$$\theta_w = (1 - \delta - \epsilon)^{N_w}$$

since the x-plane eigenvalue of the working phase is exactly $(1 - \delta - \epsilon)^{-1}$.

30

SYNTHESIS

Now we shall suggest an answer to the following question: For any given two-mode process, how may the train-work cycle be designed? In particular, if the train-work cycle is of the form shown in Figure 17, how should N_t, N_w, N_r be chosen?

Suppose we want the success probability $z(n)$ to remain above a certain prescribed value ζ_L. In that event Equations 96 and 97 will enable us to find N_t, N_w, and N_r. (Hereafter we shall refer to any triplet N_t, N_w, N_r as a "train-work schedule.")

By our assumption that the training phase contains only one nonconstant eigenfunction, the training success probability is approximately of the form

$$z(n) = \zeta - \left[\zeta - z(N_t - N_r)\right]\xi_r^{-n} \tag{99}$$

for

$$N_t - N_r \leq n \leq N_t$$

where ξ_r is the smallest nonunity x-plane eigenvalue of the training phase. Under the Two-Mode Example on page 35, we shall show how ξ_r may be estimated.

Choosing N_r: In the next section we shall show that making N_r as small as possible will maximize the ratio of working time to retraining time, N_w/N_r. Hence N_r either will be unity or certain practical factors will force us to choose N_r larger than unity. In any event, N_r will be known at the beginning of the design process.

Finding θ_r: We can find θ_r in terms of N_r and ξ_r. Recall that $\theta_r = b_t/a_t$, referring to Figure 17. This fact, together with Equation 99 yields

$$\theta_r = \xi_r^{-N_r} \tag{100}$$

Choosing N_t: We should choose a value of N_t that will yield as small a rise time as possible in the performance wave, and will also result in a minimal amount of motion of the valleys in $z(n)$ as n progresses from one work-retrain cycle to the next. To achieve these goals, we suggest that $z(n)$ be computed sequentially for n = 0, 1, 2, ... until we find the smallest n such that

$$z(n - N_r + 1) > \zeta_L \tag{101}$$

Set this value of n equal to N_t.

The next step is to find $\hat{\zeta}_L$. To do this we substitute the desired value of ζ_L in Equation 94. This equation also requires ζ and ζ_F. The value of ζ may be found either from an exact analysis of the training wave, $z(n)$, or from a weak-coupling analysis. In the latter analysis, Equation 44 yields an estimate of ζ.

Finding ζ_F: To find ζ_F, use Equations 85 and 83. For Equation 83, we may find $\hat{r}_A(0)$ and $\hat{r}_B(0)$ either exactly (by Equation 11) or approximately by the equations

31

$$\hat{\underline{r}}_A(n) \cong \hat{\underline{r}}_{A_0}(n) = \hat{\underline{r}}_A(0) \, \underline{A}^n$$

$$\hat{\underline{r}}_B(n) \cong \hat{\underline{r}}_{B_0}(n) = \hat{\underline{r}}_B(0) \, \underline{B}^n$$

$$\left. \right\} \qquad (102)$$

(These vectors had to be computed when we computed the training phase performance wave for choosing a value of N_t.)

Finding ζ: To find ζ, we may use the method under Infinite Training on page 12. We realize that even if ζ_F is computed on the basis of the exact training performance wave, obtained from Equation 11, the computed value of ζ_F is not quite equal to the ζ_F associated with the limiting working phase as $n \to \infty$. We believe, however, that the approximation is good enough for the purpose of finding a train-work schedule that will achieve a desired ζ_L. This belief is supported by the numerical example under Two-Mode Example — Part 2 on page 35.

Finding θ_w: Once ζ and ζ_F — or estimates of them — are obtained, we may compute the desired value of $\hat{\zeta}_L$ from Equation 94. This value of $\hat{\zeta}_L$, together with Equation 96 yields an estimate of θ_w. An explicit expression for θ_w, based on Equation 96, is

$$\theta_w = \frac{\hat{\zeta}_L}{1 - \theta_r(1 - \hat{\zeta}_L)} \qquad (103)$$

All that remains is the computation of N_w.

Finding N_w: We see in Equation 87 that the reciprocal of the working-phase x-plane pole is

$$\xi_w^{-1} = 1 - \delta - \epsilon \qquad (104)$$

Now

$$\theta_w = \xi_w^{-N_w}$$

Hence

$$N_w = \log_{\xi_w^{-1}}(\theta_w) \equiv \log_{\xi_w}(\theta_w^{-1})$$

This completes the computation of the training schedule.

The above procedure is summarized by the following equation, whose derivation we leave to the reader:

$$N_w = \log_b \left[\frac{\hat{\zeta}_L}{1 - \theta_r(1 - \hat{\zeta}_L)} \right] \qquad (105)$$

where

$$b \overset{\Delta}{=} \xi_w^{-1} = 1 - \delta - \epsilon, \qquad \theta_r \overset{\Delta}{=} \xi_r^{-N_r}, \qquad \hat{\zeta}_L \overset{\Delta}{=} \frac{\zeta_L - \zeta_F}{\zeta - \zeta_F} .$$

32

MAXIMIZING THE WORK RATIO

We shall demonstrate that, for a specified ζ_L, the ratio N_w/N_r is maximized when $N_r = 1$. If for special reasons N_r must be larger than 1, then the ratio N_w/N_r — which we call the "work ratio" — is maximized when N_r is as small as possible. This property is subject to the assumptions of the RC-Circuit Approximation (page 29).

Construct two sets of contours in the $\theta_r \theta_w$-plane: a) $\hat{\zeta}_L$ contours and b) N_w/N_r contours, normalized with respect to ξ_r and ξ_w.

The $\hat{\zeta}_L$ contours, found directly from Equation 103, are shown in Figure 19.
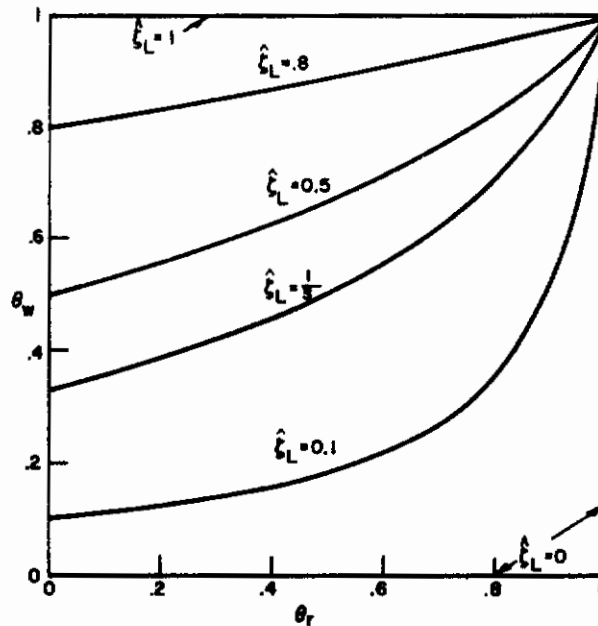
Figure 19. $\hat{\zeta}_L$ Contours.

The N_w/N_r contours are found by the following reasoning:

$$\theta_r = \xi_r^{-N_r}, \quad \theta_w = \xi_w^{-N_w} \tag{106}$$

Hence

$$\theta_w = \theta_r^W \tag{107}$$

where

$$W \triangleq \frac{N_w}{N_r} \log_{\xi_r} (\xi_w) \tag{108}$$

Thus W is the ratio N_w/N_r normalized with respect to ξ_w and ξ_r. Hence N_w/N_r is maximized whenever W is maximized, since ξ_r and ξ_w are invariants of any given process. The W contours, found from Equation 107, are shown in Figure 20.

33
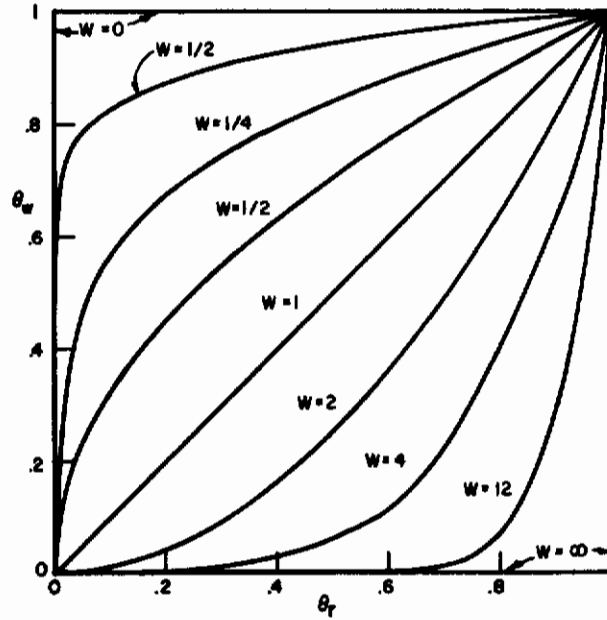
Figure 20. W Contours.

For any particular ζ_L, the value of $\hat{\zeta}_L$ will be fixed, by the assumptions of the RC-Circuit Approximation (page 29). Hence for any desired ζ_L, the attainable pairs (θ_r, θ_w) must lie on one of the $\hat{\zeta}_L$ contours in Figure 19. To maximize N_w/N_r, we must choose that point on the $\hat{\zeta}_L$ contour which yields the largest value of W. To find this point we may superpose the W contours on the $\hat{\zeta}_L$ contours. When we do this we find that for every fixed $\hat{\zeta}_L$, the greatest W is achieved when $\theta_r = \theta_w = 1$. We also find that a curve of W versus θ_r for any fixed $\hat{\zeta}_L$ is monotonically increasing. Hence N_w/N_r versus θ_r for any fixed ζ_L will be monotonically increasing — provided, of course, that the RC-Circuit Approximation (page 29) holds true.

The fact that the work ratio is a maximum at $\theta_r = \theta_w = 1$ raises the following question: What is a formula for the work ratio at $\theta_r = 1$? To answer this, note that Equations 108 and 107 yield the following formula:

$$\frac{N_w}{N_r} = W \log_{\xi_w} (\xi_r) \tag{109}$$

where

$$W \overset{\Delta}{=} \log_{\theta_r} (\theta_w) \tag{110}$$

Unfortunately, Equation 110 is indeterminate at $(\theta_r, \theta_w) = (1, 1)$. To find W at $\theta_r = \theta_w = 1$, find the partial derivatives with respect to θ_r of Equations 103 and 107 at $\theta_r = 1$. Putting the two resulting expressions equal to each other yields $W = \hat{\zeta}_L^{-1} - 1$. Hence

$$\left(\frac{N_w}{N_r} \right)_{max} = \left(\frac{N_w}{N_r} \right)_{\theta_r = 1} = \left(\frac{1}{\hat{\zeta}_L} - 1 \right) \log_{\xi_w} (\xi_r). \tag{111}$$

This expression is a convenient way of estimating the maximum possible work ratio of a two-mode system, subject to the assumptions of the RC-Circuit Approximation (page 29). A more accurate formula, of course, is given by Equation 105, in which we would set N_r equal to the smallest achievable value, which would be unity, barring special practical considerations. Equation 111, however, is a convenient approximation.

34

7. A TWO-MODE EXAMPLE - PART 2.

The foregoing techniques will be illustrated, using a two-mode TLP of the type discussed under Part 1 (page 13). We shall examine a two-mode TLP whose distinguishing parameters are $a = 0.6$, $\rho = 0.9$, and $\delta = \epsilon = 0.01$, where a and ρ are defined by Equations 45 and 46. The point $(a, \rho) = (0.6, 0.9)$ lies well within the shaded region of Figure 9. This ensures that any working-phase asymptote ζ_F will be significantly different from the training phase asymptote ζ. The small values of δ and ϵ will permit us to use the weak-coupling approximations. We shall assume throughout this discussion that the initial threshold is at $k = 1$.

THE TRAINING PERFORMANCE WAVE

The success probability during training, which we call the "training performance wave," may be obtained from the weak-coupling approximation, Equation 43. We repeat this equation here, adding $\tilde{z}(n)$ as a definition of the right member:

$$z(n) \cong \tilde{z}(n) \triangleq \gamma z_{Ao}(n) + (1-\gamma) z_{Bo}(n) \tag{112}$$

where

$$\gamma \triangleq \frac{\epsilon}{\delta + \epsilon} \tag{113}$$

Since $\delta = \epsilon$, we have

$$\gamma = \frac{1}{2}. \tag{114}$$

The constituent one-mode training performance waves, $z_{Ao}(n)$ and $z_{Bo}(n)$, are found as follows:

$$z_{Ao}(n) = \hat{\underline{r}}_A(0) \underline{A}^n \underline{q}_{Ao} \tag{115}$$

$$z_{Bo}(n) = \hat{\underline{r}}_B(0) \underline{B}^n \underline{q}_{Bo} \tag{116}$$

where

$$\hat{\underline{r}}_A(0) = \hat{\underline{r}}_B(0) = (1, 0, 0) \tag{117}$$

$$\underline{A} = \begin{bmatrix} 0.1 & 0.9 & 0 \\ 0 & 1 & 0 \\ 0 & 0.1 & 0.9 \end{bmatrix} \tag{118}$$

$$\underline{B} = \begin{bmatrix} 0.280 & 0.720 & 0 \\ 0.020 & 0.800 & 0.180 \\ 0 & 0.080 & 0.920 \end{bmatrix} \tag{119}$$

35

The elements of $\underline{B}$ were computed in accordance with Table 1 of ref. 2. The pertinent portion of this table is repeated here:

$$b_{11} = 1 - \frac{\rho}{2}(1+a) \qquad b_{12} = \frac{\rho}{2}(1+a) \qquad b_{13} = 0$$

$$b_{21} = \frac{1-\rho}{2}(1-a) \qquad b_{22} = \frac{1}{2}(1+a) \qquad b_{23} = \frac{\rho}{2}(1-a) \tag{120}$$

$$b_{31} = 0 \qquad\qquad b_{32} = \frac{1-\rho}{2}(1+a) \qquad b_{33} = \frac{1}{2}(1-a) + \frac{\rho}{2}(1+a)$$

When $(a, \rho) = (0.6, 0.9)$ are substituted in the above formulas, the element values in Equation 119 are obtained.

The elements of q_{Ao} and q_{Bo} are just the diagonal elements of $\underline{A}$ and $\underline{B}$ (for this particular example):

$$q_{Ao} = \{0.1 \quad 1 \quad 0.9\} \tag{121}$$

$$q_{Bo} = \{0.280 \quad 0.800 \quad 0.920\} \tag{122}$$

where the braces indicate column vectors. Equations 112 to 122 yield the function $\tilde{z}(n)$, which is plotted in Figure 21. This function will now be compared to the exact performance wave $z(n)$.
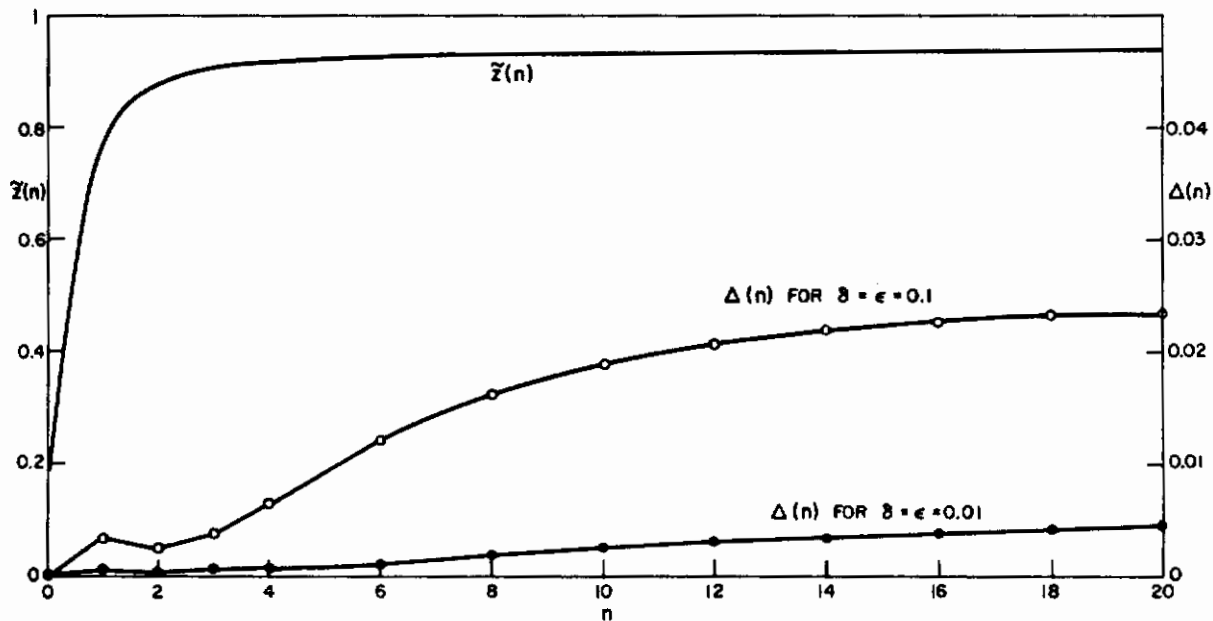

Figure 21. Training Performance Wave of Numerical Example.

The latter is found as follows:

$$z(n) = \underline{r}(0)\,(\underline{\Gamma}\,\underline{P})^n\,\underline{q}$$

36

where $\quad \underline{r}(0) = [0.5 \quad 0 \quad 0 \quad 0.5 \quad 0 \quad 0]$

$$\underline{\Gamma} = \begin{bmatrix} 1-\delta & \delta \\ \epsilon & 1-\epsilon \end{bmatrix}$$

$$\underline{P} = \begin{bmatrix} \underline{A} & \underline{0} \\ \underline{0} & B \end{bmatrix}$$

$$\underline{0} = \begin{bmatrix} 0 & 0 & 0 \\ 0 & 0 & 0 \\ 0 & 0 & 0 \end{bmatrix}$$

$\underline{A}$ and $\underline{B}$ are given by Equations 118 and 119. The column vector $\underline{q}$ consists of two column vectors $\underline{q}_A$ and $\underline{q}_B$:

$$\underline{q} = \begin{bmatrix} \underline{q}_A \\ \underline{q}_B \end{bmatrix} \tag{123}$$

where $\underline{q}_A$ and $\underline{q}_B$ are given in terms of $\underline{q}_{Ao}$ and $\underline{q}_{Bo}$ in Equation 37. The column vectors $\underline{q}_{Ao}$ and $\underline{q}_{Bo}$ are, in turn, given by Equations 121 and 122.

The resulting function $z(n)$ is so close to $\widetilde{z}(n)$ that no difference between the two would be visible in Figure 21. To make this difference visible, the difference $\Delta(n) \overset{\Delta}{=} \widetilde{z}(n) - z(n)$ is plotted in Figure 21 on a magnified scale. The curve is marked "$\Delta(n)$ for $\delta = \epsilon = 0.01$." Note that $\Delta(n)$ approaches its maximum as $n \to \infty$, and that $\Delta(\infty) = 0.004$.

THE WORKING PERFORMANCE WAVE AFTER INFINITE TRAINING

To find any working performance wave, we need three parameters in conjunction with Equation 88: $z_F(0)$, ζ_F, and $\delta + \epsilon$, where the quantity $z_F(0)$ is the success probability at the initial instant of the working phase.

Consider the problem of finding the working performance wave after the two-mode TLP has been trained for a long time, or — speaking mathematically — finding the working performance wave when the initial threshold probability vector is identical to the limit as $n \to \infty$ of the threshold probability vector during a training phase.

To solve this problem, we shall use Equations 85 and 86. These equations require the computation of ψ_A, ψ_B, ψ_{AB}, and ψ_{BA} at the end of the training phase. Hence, by Equation 83, we must know $\hat{r}_A(n)$ and $\hat{r}_B(n)$ at the end of the training phase, i.e., we must know $\hat{r}_A(\infty)$. ($\hat{r}_A(n)$ and $\hat{r}_B(n)$ are equal to $\hat{r}_A(0)$ and $\hat{r}_B(0)$ in Equation 83, because of the shift in the time origin.)

37

Using the weak-coupling approximation, we shall assume that

$$\hat{\underline{r}}_A(\infty) \cong \hat{\underline{r}}_{Ao}(\infty)$$

$$\hat{\underline{r}}_B(\infty) \cong \hat{\underline{r}}_{Bo}(\infty)$$

Merely by inspection of the state transition graph of mode $\underline{A}$ (Figure 22), we find that

$$\hat{\underline{r}}_{Ao}(\infty) = [0, 1, 0]. \tag{124}$$
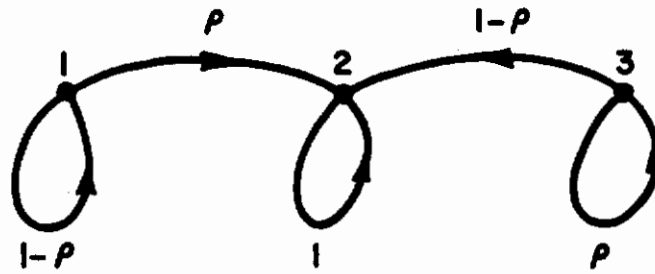
Figure 22. The State Transition Graph for Mode $\underline{A}$ in the Numerical Example.

To find $\hat{r}_{Bo}(\infty)$, we use Kaplan's method. Figure 23 shows the state transition graph of mode $\underline{B}$. The values of the transition probabilities in this graph are given by Equation 119.
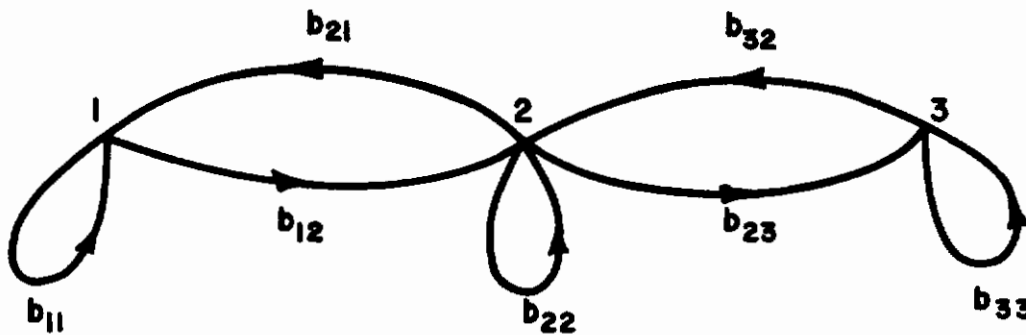
Figure 23. The State Transition Graph of Mode $\underline{B}$.

Using Kaplan's method, node 2 of Figure 23 is split into two nodes: a "source" and a "sink." A unit impulse is applied to the source node. The resulting graph is shown in Figure 24. Denote the "total" signals at nodes 1 and 3 by σ_1 and σ_3, respectively. Then an inspection of Figure 24 yields

$$\sigma_1 = \frac{b_{21}}{1 - b_{11}} = 0.0278$$

$$\sigma_3 = \frac{b_{23}}{1 - b_{33}} = 2.2500$$
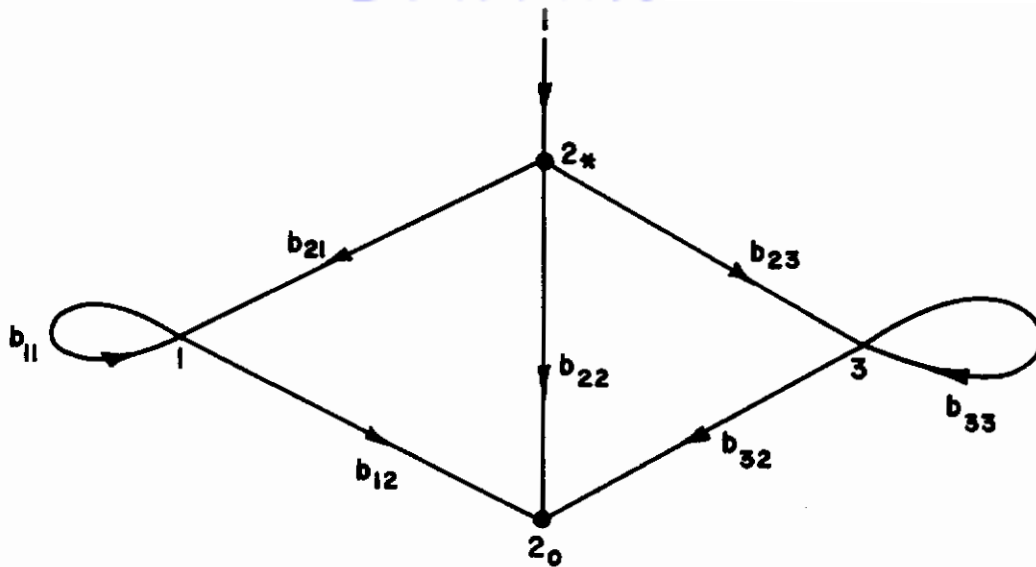
Figure 24. The Modified State Transition Graph for Computing
$\hat{\underline{r}}_{Bo}(\infty)$ by Kaplan's Method.

Total delay $\overset{\Delta}{=} d = 1 + \sigma_1 + \sigma_3 = 3.2778$. Hence

$$\underline{r}_{Bo}(\infty) = \left[\frac{\sigma_1}{d} \quad \frac{1}{d} \quad \frac{\sigma_3}{d} \right]$$

$$= [0.0085 \quad 0.3051 \quad 0.6864].$$

The values of $\underline{q}_{Ao}$ and $\underline{q}_{Bo}$ are given by Equations 121 and 122. Hence, using Equation 83 together with the weak-coupling approximation we have

$$\psi_A \cong \hat{\underline{r}}_{Ao}(\infty) \, \underline{q}_{Ao} = 1$$

$$\psi_B \cong \hat{\underline{r}}_{Bo}(\infty) \, \underline{q}_{Bo} = 0.8780$$

$$\psi_{AB} \cong \hat{\underline{r}}_{Ao}(\infty) \, \underline{q}_{Bo} = 0.800 \tag{125}$$

$$\psi_{BA} \cong \hat{\underline{r}}_{Bo}(\infty) \, \underline{q}_{Ao} = 0.9237$$

Since $\delta = \epsilon = 0.01$, we have $\gamma = \frac{1}{2}$. Hence, by Equation 85,

$$\zeta_F \cong \tilde{\zeta}_F \overset{\Delta}{=} \frac{1}{4} (\psi_A + \psi_B + \psi_{AB} + \psi_{BA}) = 0.9004 \tag{126}$$

39

By Equatioon 86, the beginning of the working cycle is

$$z_F(0) = \zeta \cong \tilde{\zeta} \triangleq \frac{1}{2}(\psi_A + \psi_B) = 0.9390. \tag{127}$$

Substituting Equations 126 and 127 in **Equation 88 and recalling that** $\delta + \epsilon = 0.02$, we obtain

$$z_F(n) \cong 0.9004 + (0.0386)(0.98)^n \tag{128}$$

as the working performance wave.

To check the accuracy of Equation 128, **we need only compute** ζ and ζ_F by exact methods. This was done on a digital computer, using the **exact method described under** "The Training Performance Wave" (page 35). The results are:

$$\zeta = 0.93429705$$

$$\zeta_F = 0.90038880$$

Hence, within four decimal places,

$$\tilde{\zeta} - \zeta = 0.0004$$

and

$$\tilde{\zeta}_F - \zeta_F = 0.0000$$

Hence the error in Equation 128 never exceeds 0.0004.

THE DISTANCE BETWEEN ζ AND ζ_F

At first it may seem surprising that ζ and ζ_F differ by only about four percent even though $(a, \rho) = (0.6, 0.9)$ falls well within the shaded region of Figure 9. This means that the working phase in the present example imposes only a small deterioration on the success probability. Hence for this case no retraining would be needed from a practical viewpoint. The question arises: Under what circumstances will ζ_F differ substantially from ζ? We suggest that this will occur when the number of available thresholds, K, is larger than 3. Intuition tells us that when K is large it will be possible to reduce the "cross-correlations" ψ_{AB} and ψ_{BA}. (Recall that if $\psi_{BA} = \psi_{BA} = 0$ and if $\gamma = \frac{1}{2}$, then $\zeta = 2\zeta_F$.) This conjecture needs to be substantiated by an analysis of K-threshold two-mode processes with K > 3.

TRAIN-WORK SCHEDULES

We shall synthesize a number of train-work schedules with a design goal of

$$\zeta_L \cong 0.9250 \tag{129}$$

Note that the above value of ζ_L is slightly more than half the distance from ζ_F to ζ,

The train-work schedule will consist of a training interval N_t, followed by N_w, N_r, N_w, N_r, ..., as in Figure 17. In accordance with the procedure outlined on page 31, we first compute ξ_r^1, where ξ_r is the smallest nonunity x-plane eigenvalue of the training phase. First we find ξ_{Ar}^1, which is the ξ_r^1 for mode A alone. This may be found from an inspection of Figure 22:

$$\underline{r}(x) = \left[\frac{1}{1 - (1-\rho)x} , \frac{\rho x}{[1-(1-\rho)x](1-x)} , 0 \right]$$

Hence

$$\xi_{Ar}^{-1} = 1 - \rho = 0.1$$

Then one finds ξ_{Br}^{-1} by one of two methods. In one method, we use the ν contours of mode $\underset{\sim}{B}$. These contours, which were given in an earlier paper [ref. 2], are reproduced in Figure 25. In this figure,
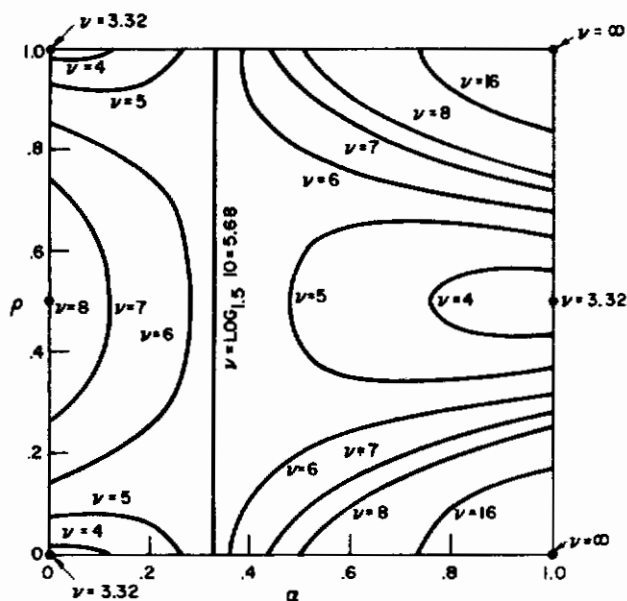
Figure 25. ν Contours for Mode $\underset{\sim}{B}$.

we find at $(a,\rho) = (0.6, 0.1)$ that $\nu_{Bo} = 8$. Hence

$$\xi_{Br}^{-1} = (0.1)^{\frac{1}{8}} = 0.750. \tag{130}$$

The second method is more accurate. It makes use of an explicit formula for ξ_{Br}^{-1}, obtained from the characteristic equation associated with mode $\underset{\sim}{B}$. This formula is

$$\xi_{Br}^{-1} = \frac{Y}{1 - \sqrt{1-2Y}}$$

where

$$Y \triangleq \frac{1+a}{2} [1 - a + \rho(1-\rho)(3a-1)]. \tag{131}$$

41

For $(a, \rho) = (0.6, 0.9)$, Equation 131 yields

$$\xi_{Br}^{-1} = 0.749 \qquad (132)$$

Since $\gamma = \frac{1}{2}$, both ξ_{Ar} and ξ_{Br} play a part in the two-mode performance wave. When the performance wave is near its asymptote, however, only the smaller of ξ_{Ar} and ξ_{Br} dominates the performance wave. Hence

$$\xi_r^{-1} = \text{Max} \left(\xi_{Ar}^{-1}, \xi_{Br}^{-1}\right) = 0.749. \qquad (133)$$

Next we compute N_t. To do this, we use Equation 101 in conjunction with the training performance wave computed earlier (Figure 21), setting $N_r = 1$. This yields

$$N_t = 6. \qquad (134)$$

Later we shall try other values of N_r. Remember, however, that $N_r = 1$ is the optimum choice when it is achievable.

We compute $\hat{r}_A(N_t)$ and $\hat{r}_B(N_t)$, using

$$\left. \begin{array}{l} \underline{r}_A(N_t) = \begin{bmatrix} 1 & 0 & 0 \end{bmatrix} \underline{A}^{N_t} \\[2em] \underline{r}_B(N_t) = \begin{bmatrix} 1 & 0 & 0 \end{bmatrix} \underline{B}^{N_t} \end{array} \right\} \qquad (135)$$

where $\underline{A}$ and $\underline{B}$ are given by Equations 118 and 119. We then find the ψ's by Equation 125, replacing $\hat{r}_{Ao}(\infty)$ and $\hat{r}_{Bo}(\infty)$ by $\hat{r}_{Ao}(N_t)$ and $r_{Bo}(N_t)$, respectively. This yields, for $N_t = 6$,

$$\left. \begin{array}{l} \psi_A(6) = 1.0000 \\[1em] \psi_B(6) = 0.8523 \\[1em] \psi_{AB}(6) = 0.8000 \\[1em] \psi_{BA}(6) = 0.9349 \end{array} \right\} \qquad (136)$$

Hence, by Equation 86, the training performance at $n = N_t$ is

$$z(6) = z_F(0) \cong \gamma \, \psi_A(6) + (1 - \gamma) \, \psi_B(6) \qquad (137)$$

Furthermore the asymptotic performance of a working phase starting at $n = 6$ is

$$\zeta_F(6) \cong \gamma^2 \, \psi_A(6) + (1 - \gamma)^2 \, \psi_B(6) + \gamma(1 - \gamma)[\psi_{AB}(6) + \psi_{BA}(6)]. \qquad (138)$$

Setting $\gamma = \frac{1}{2}$ and substituting Equations 136 in Equations 137 and 138 yields

$$z(6) \cong 0.9262 \qquad (139)$$

$$\zeta_F(6) \cong 0.8968 \qquad (140)$$

42

(Actually, it was unnecessary to compute $z(6)$, since we had already computed it when we found $N_t = 6$ by Equation 101. We included the recomputation of $z(6)$ for illustrative purposes only.)

In a preceding section we computed the value of ζ using the weak-coupling approximation (Equations 125 and 127). The result was

$$\zeta \cong 0.9390. \qquad (141)$$

Next we find θ_r for $N_r = 1$. Using Equations 100 and 133, we find that

$$\theta_r = \xi_r^{-1} = 0.749. \qquad (142)$$

Next we find $\hat{\zeta}_L$, substituting Equations 129, 140, and 141 in Equation 94. This yields

$$\hat{\zeta}_L = 0.665 \qquad (143)$$

By Equation 104,

$$\xi_w^{-1} = 0.98 \qquad (144)$$

Substituting Equations 142, 143, 144 in Equation 105 yields

$$N_w \cong 5.90$$

The nearest integer to 5.90 is 6. Hence we choose

$$N_w = 6.$$

Summarizing: The train-work schedule we have designed is $(N_t, N_w, N_r) = (6, 6, 1)$.

By using other values of N_r, we can obtain other train-work schedules having the same design goal of $\zeta_L = 0.9250$. Examples of such schedules are listed in Table 1.

TABLE 1

*SEVERAL SCHEDULES ACHIEVED BY SYNTHESES IN WHICH
THE DESIRED ζ_L IS 0.9250.*

Train-Work Schedule			Work Ratio	Estimated	Actual
N_t	N_w	N_r	N_w/N_r	ζ_L	ζ_L
	0	0	7.10		
6	6	1	6	0.9249	0.9201
7	10	2	5	0.9248	0.9202
9	15	4	3.75	0.9246	0.9206
12	18	7	2.57	0.9249	0.9215
15	19	10	1.90	0.9250	0.9221
25	20	20	1		
∞	20	∞	0		

The fourth column in this table lists the work ratio N_w/N_r for each schedule. Included in this column is the train-work ratio at $N_w = N_r = 0$, obtained by Equation 111. Note that, as predicted, the work ratio decreases monotonically as the retraining time increases.

43

Suppose $\delta = \epsilon = 0.1$, rather than 0.01 as in the original example. Here, $\xi_w = (1-0.2)^{-1} = 1.25$. When $\delta = \epsilon = 0.01$, we have $\xi_w = 1.0204$. Hence, by Equation 111, the maximum work ratio for $\delta = \epsilon = 0.1$ is 7.10 (i.e., the maximum work ratio for $\delta = \epsilon = 0.01$) divided by $\log_{1.0204}(1.25)$. We find that $\log_{1.0204}(1.25 = 11.03$. Consequently, raising δ and ϵ from 0.01 to 0.1 gives a ratio of 0.644, which indicates an inefficient training situation. In fact, Equation 111 tells us that to achieve $\zeta_L \geq 0.925$ with a work ratio exceeding unity, the value of $\delta + \epsilon$ must be less than 0.154. Hence, if $\delta = \epsilon$, δ must lie below 0.077 in order to achieve $\zeta_L = 0.925$ with a work ratio exceeding unity. Thus we see here how Equation 111 gives us an easy way to estimate the effect of parameter changes on the work ratio and vice versa.

EVALUATION OF THE WEAK-COUPLING APPROXIMATION

In order to examine the validity of the weak-coupling approximation, the exact training performance wave was computed for the case where $\delta = \epsilon = 0.1$, everything else remaining as before. The resulting error curve, marked "$\Delta(n)$ for $\delta = \epsilon = 0.1$" is shown in Figure 21. Again the error curve is monotonically increasing, except for a small dip near the origin, and is similar in shape to the error curve for the first case, $\delta = \epsilon = 0.01$. However, the asymptotic error of the second curve is only about five times greater than that of the first curve, even though at $n = 1$ the second error is about ten times the first.

Since the error curves in Figure 21 suggest that the maximum value of $\Delta(n)$ occurs at $n = \infty$ independently of δ, we computed $\Delta(\infty)$ for several values of δ, assuming $\delta = \epsilon$. The results are plotted in Figure 26. Note that in the range $0 \leq \delta \leq 0.1$, the error remains below 2.5 percent.
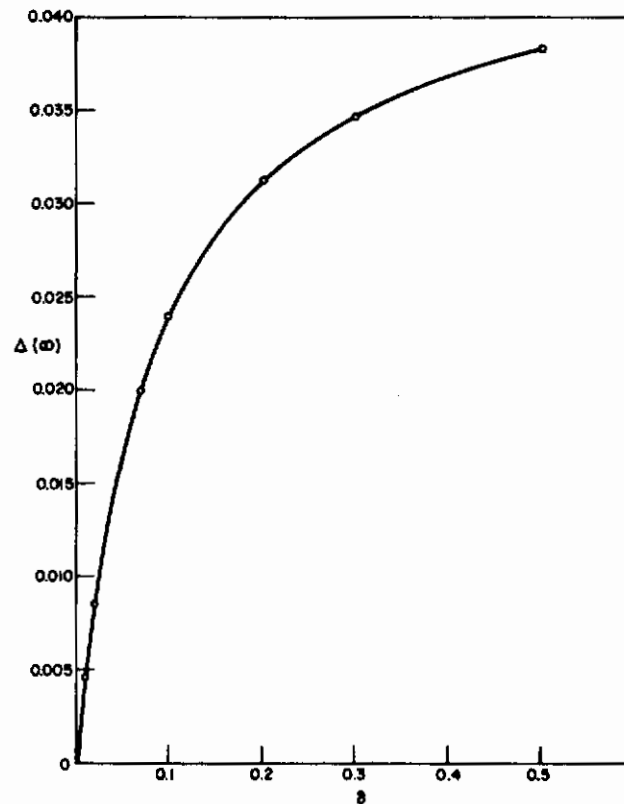

Figure 26. Asymptotic Error of the Weak-Coupling Approximation as a Function of the Coupling Strength.

44

On the other hand recall from the numerical example that in order to achieve a reasonable ζ_L with a work ratio exceeding unity, the value of δ had to be less than 0.077, assuming $\delta = \epsilon$. A work ratio of less than unity seems to be unsatisfactory, because in most training situations in every-day experience, the duration of the work growing out of a training program is substantially greater than the training time.

Recapitulating: In the present numerical example, reasonable performance (we assume $\zeta_L \geq 0.925$ is reasonable) with reasonably large work ratios can be achieved only if the mode-to-mode transition probability δ lies in the range $0 \leq \delta \leq 0.1$. For this range of δ the maximum error of the weak-coupling approximation lies below 2.5 percent.

These numerical results suggest that the weak-coupling approximation will be valid when-ever the coupling is weak enough to permit reasonable values of ζ_L to be achieved by work ratios greater than unity. Further evidence, however, is needed to establish the generality of this sug-gestion.

EVALUATION OF THE RC-CIRCUIT APPROXIMATION

To evaluate the effectiveness of the synthesis procedure, we computed on a digital computer the actual values of ζ_L, using an exact analysis (page 26) for five of the train-work schedules. These values of ζ_L are listed in the last column of Table 1. For comparison, the estimated values of ζ_L obtained by the RC-circuit approximation are listed in the fifth column. These estimated values are not quite equal to the design goal of 0.9250, because of the unavoidable roundoff in N_w. An inspection of these results shows that in every schedule the design error for ζ_L is less than 0.55 percent.

It is possible to improve the accuracy of the synthesis by using the exact training per-formance wave instead of the weak-coupling approximation of the training performance wave. Of course the RC-circuit approximations (page 29) are retained to keep the synthesis procedure within reasonable manageability. The results of this technique, using the same design goal of $\zeta_L = 0.9250$, are summarized in Table 2.

TABLE 2

SEVERAL IMPROVED SCHEDULES ACHIEVING $\zeta_L \cong 0.9250$.

Train-Work Schedule			Work Ratio	Actual
N_t	N_w	N_r	N_w/N_r	ζ_L
7	5	1	5	0.9217
8	8	2	4	0.9222
10	12	4	3.75	0.9227
13	15	7	2.29	0.9231
16	16	10	1.60	0.9236
26	16	20	0.80	
∞	16	∞	0	

The estimated values of ζ_L were not computed in this table, because we saw in Table 1 that the roundoff in N_w has negligible effect on the estimated ζ_L. The actual ζ_L's of Table 2 are compared to those of Table 1 in Figure 27. In this figure, we see that approximately half of the error is eliminated by using the exact training performance wave as part of the synthesis procedure.
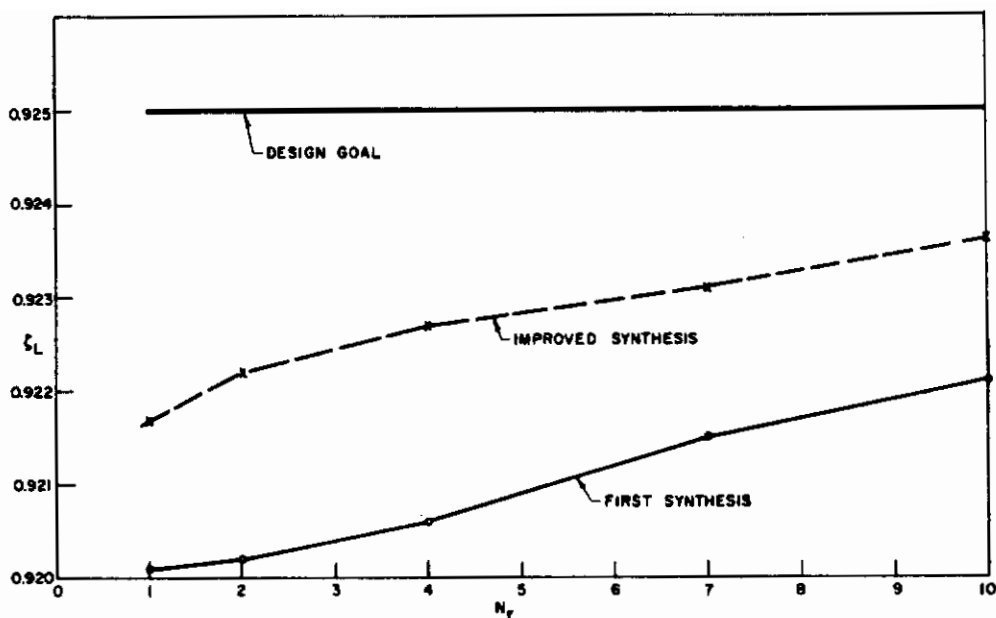
Figure 27. A Comparison of the ζ_L's Achieved by the Two Sets of Train-Work Schedules.

Recapitulating: In this numerical example, the RC-circuit approximation for synthesizing train-work schedules yields errors in ζ_L of less than 0.55 percent when $\delta = \epsilon = 0.01$. These errors are cut by about one-half by using the exact training performance wave as part of the synthesis procedure.

To test further the validity of the assumptions of the RC-circuit approximation (page 29), we computed the exact value of ζ_L for a few different values of N_t, keeping N_w and N_r fixed at $N_w = 6$, $N_r = 1$. The results are given in Table 3.

TABLE 3

EFFECT OF CHANGING N_t.

(Desired $\zeta_L = 0.9250$)

Train-Work Schedule			Actual
N_t	N_w	N_r	ζ_L
3	6	1	0.9209
6	6	1	0.9201
7	6	1	0.9202
16	6	1	0.9200

We note that the effect of a change in N_t has a very small effect on ζ_L — only about 0.01% when $N_t >$ optimum value. If $N_t <$ optimum value, the effect is less than 0.1%. We conclude that the effect of N_t on ζ_L is negligible, which lends support to the RC-circuit model as an acceptable approximation of the train-work cycle.

46

8. MODELING ADAPTIVE PROCESSES IN THE LIFE SCIENCES

In most adaptive processes in the life sciences, no obvious model of the process exists. In particular, the random walk associated with one-mode TLPs will not necessarily be a good model of a given biological process. A very important need, therefore, is a technique for determining a good model from a limited number of experiments.

This report, together with the preceding paper [ref. 2], points toward methods of modeling adaptive processes by Markov chains. One such method involves a comparison of the open-loop and closed-loop performances. In particular, the ζ_M contours are computed from the open-loop performance, and the ζ contours are computed from the closed-loop performance. If the contours are similar to those in Figure 9, and if in addition the transient performance wave is monotonic, a random walk model shows promise of being appropriate.

In some biological or psychological processes, a two-mode model may be preferable to a one-mode model. Suppose, for example, that a discrimination learning task involving a sequence of training stimuli extends over a period of several hours, that each element of the sequence consists of a string of 20 bits, and that the trainee is a human being. Under these conditions, the trainee's attention span may fluctuate between a short span of about 5 bits and a long span of about 15 bits. To test the hypothesis that the trainee's attention span fluctuates between two string lengths, we need a way of distinguishing one-mode from two-mode processes.

One way to make this distinction is by examining the contours of ζ and ζ_M.* In a one-mode process, each ζ_M contour is everywhere inside the corresponding ζ contour, and the two contours never intersect. In a two-mode process, each ζ_M contour intersects with the corresponding ζ contour in the manner shown in Figure 9. Since the ζ_M contours are composites of the open-loop contours (i.e., the ζ_k contours), the relations between the open-loop and closed-loop behaviors can help us decide between a one-mode and a two-mode model for a particular adaptive process.

Another way of distinguishing one-mode from two-mode (or N-mode) processes is to inspect the statistics of a working phase. If the working-phase performance wave decreases monotonically, the process is likely to require a N-mode model rather than a one-mode model for an adequate description of its behavior.

---

*To find ζ_M contours of a human observer, train him to use a specific threshold in discriminating between the two classes of signals. Then permit him to operate in an open-loop condition. This yields a set of ζ_k contours for a specific k. Repeat the training to achieve a new value of k. After all the ζ_k maps are acquired, find ζ_M via $\zeta_M = \underset{k}{\text{Max}} \, (\zeta_k)$.

9. SUMMARY AND OUTLOOK

In this section the preceding chapters are summarized, and extensions of the present work are suggested.

EXACT ANALYSIS OF TWO-MODE PROCESSES

A two-mode process is exactly analyzable by a Markov chain, even when the coupling is strong. Furthermore the behavior of the process is exactly describable in terms of the matrices of the constituent one-mode processes and the parameters of the mode-to-mode fluctuations.

From one point of view this is surprising. A two-mode process or, more generally, an N-mode process can be viewed as a Markov chain whose transition probabilities are subject to random fluctuations among N sets of transition probabilities. Consequently an N-mode process can be viewed as a nonstationary Markov chain. We have shown that this particular type of nonstationary Markov chain is representable by a stationary Markov chain!

THE WEAK-COUPLING APPROXIMATION

The performance wave (i.e., the success probability as a function of time) of any two-mode process may be approximated as a linear sum of the constituent one-mode performance waves (Equations 43 and 44). The errors of this approximation are small when $\delta \ll 1$, $\epsilon \ll 1$. Hence this is called a weak-coupling approximation. The errors of the approximation approach a maximum as the number of trials, n, becomes indefinitely large. These asymptotic errors, however, remain small when $\delta \ll 1$, $\epsilon \ll 1$. In the numerical example of the preceding chapter the asymptotic errors remain below 2.5 percent when $0 \leq \delta \leq 0.1$, $\delta = \epsilon$.

Future Work: In order to evaluate the utility of the weak-coupling approximation and to determine where its application is appropriate, a general error analysis of the approximation should be made. In addition, an attempt should be made to derive an exact expression for ζ in terms of $\underline{A}$, $\underline{B}$, δ, and ϵ.

BEST-FIXED-THRESHOLD POLICY

In a two-mode TLP the best-fixed-threshold policy can often be outperformed by a simple incremental feedback policy. Specifically, in the numerical example of a two-mode three-threshold TLP, the simple incremental feedback policy outperforms the best-fixed-threshold policy in a region covering over half of the $\alpha\rho$-square. In the remaining part of the square, a threshold fixed at $k = 2$ (the middle threshold value) outperforms the simple incremental feedback policy.

Future Work: (a) Investigate the effect of raising the number of thresholds on the size of the region over which $\zeta > \zeta_M$. Will this size be increased when the cross-correlations ψ_{AB} and ψ_{BA} are reduced? (b) Find an exact formula for γ_0 (see page 19).

ULTIMATE ASYMPTOTIC PERFORMANCE

For a two-mode TLP, the ultimate asymptotic performance realizable by any threshold policy is a linear sum of the fixed-threshold performances of the constituent one-mode TLPs (Equation 72).

48

In the case of the burst-noise channel that we studied, we found that if a change in feedback policy generates a certain stability-reliability improvement for the "bad" channel operating alone, then a proportional improvement will be obtained for the two-mode operation, with an "acceptable" region in the $a\rho$-square shaped similar to the "acceptable" region for the bad channel alone.

The contours of ultimate asymptotic performance of a two-mode process can serve as a coarse approximation of the actual asymptotic performance of the closed-loop two-mode process.

Future Work: Find out whether or not ζ_U is a *least* upper bound on the realizable asymptotic performance of a two-mode TLP.

EFFECTIVENESS OF SIMPLE INCREMENTAL FEEDBACK

The effectiveness of the simple incremental feedback policy in a weakly coupled two-mode TLP is, in the burst-noise example (page 13), greater than the effectiveness of that policy in either of the constituent one-mode processes — where effectiveness is measured as average stability-reliability improvement in the $a\rho$-plane.

WORKING PHASE PERFORMANCE

The Markov chain model permits an exact analysis of the working phase performance wave. This analysis is particularly simple, because the working phase performance wave consists of only two eigenfunctions: one is a constant and the other is the exponential function $(1 - \delta - \epsilon)^n$.

Theorem: The final success probability in a working phase of any two-mode Markov chain cannot be less than one-half of the success probability at the beginning of that phase.

In an example of a three-threshold two-mode TLP, we found that ζ and ζ_F do not differ substantially. We conjecture that they can differ substantially when the number of thresholds, K, is large.

Future Work: Investigate the above conjecture.

THE TRAINING-PHASE PERFORMANCE

The transient performance of a two-mode closed-loop process is only weakly dependent on δ and ϵ when δ and ϵ are small. On the other hand, the transient performance of a two-mode open-loop process is strongly dependent on δ and ϵ, even when δ and ϵ are small.

TRAIN-WORK CYCLES

Train-work schedules for two-mode processes may be constructed from a knowledge of the constituent one-mode behaviors. Increased accuracy in the train-work schedule may be obtained by finding the exact two-mode performance during a single training phase.

The Markov chain model yields a procedure for synthesizing train-work schedules that will realize a performance wave having a prescribed minimum value, ζ_L, after the first training phase.

Many two-mode train-work cycles can be closely simulated by the output voltage of a periodically charged and discharged resistor-capacitor circuit (Figure 18). This circuit suggests

49

the so called "RC-circuit approximation" for analyzing train-work cycles. In train-work cycles where this approximation is valid, the ratio of the working time to the retraining time (the "work ratio") is maximized when the retraining time is made as small as possible. A convenient expression for the maximum realizable work ratio is

$$\left(\frac{N_w}{N_r}\right)_{max} \cong \left(\frac{1}{\hat{\zeta}_L} - 1\right) \log_{\xi_w}(\xi_r)$$

where $\hat{\zeta}_L$, ξ_r, ξ_w are defined in Equations 94, 99, and 104.

THE NUMERICAL EXAMPLE

The analysis and synthesis techniques, in particular the weak-coupling approximation and the RC-circuit approximation, are illustrated by a numerical example. A number of train-work schedules achieving a desired minimal performance, ζ_L, were derived for a case where the coupling is $\delta = \epsilon = 0.01$. In each of these schedules, the errors in the achieved value of ζ_L was less than 0.55 percent.

The results of the numerical example suggest that the weak-coupling approximation will yield errors of the order of magnitude of 2 percent or less whenever the coupling is weak enough to permit reasonable values of ζ_L to be achieved by work ratios greater than unity.

Future Work: (a) Investigate the range of validity of the above suggestion. (b) In a future numerical example, use a pair (a, ρ) lying *outside* the region where $\zeta > \zeta_M$.

In designing train-work sequences of the form N_t, N_w, N_r, N_w, N_r, ..., the effect of N_t on the achieved value of ζ_L seems to be negligible. This enhances the applicability of the RC-circuit approximation.

In the numerical example, the RC-circuit approximation yields errors in ζ_L of less than 0.55 percent when $\delta = \epsilon = 0.01$. These errors are cut by about one-half by using the exact training performance wave in place of the weak-coupling approximation of the training performance wave as part of the synthesis procedure. A general error analysis of the RC-circuit approximation would provide a useful supplement to our work.

MODELING ADAPTIVE PROCESSES

The relations between open-loop and closed-loop behavior of adaptive processes can be helpful in finding Markov-chain models for real processes. In particular, these relations can help decide whether a one-mode or an N-mode model is appropriate. The relations of immediate interest are those between the ζ_M and ζ maps, and between the training phase and working phase. Other such relations may evolve in the future.

10. GENERAL OBSERVATIONS AND CONCLUSIONS

The Markov chain model can be used in the exact analysis of a certain class of non-stationary threshold learning processes — in particular, two-mode TLPs. As a result we find that the effectiveness of simple incremental feedback for two-mode TLPs is greater than in one-mode TLPs. This is manifested in two ways:

1. Over a substantial region of the $\alpha\rho$-plane the asymptotic success probability, ζ, of a two-mode TLP exceeds the best-fixed-threshold success probability, ζ_M. There is no such region in the case of one-mode TLPs.

2. The average stability-reliability improvement for the class of weakly coupled two-mode TLPs studied in Chapter 4 is greater than that of either of the constituent one-mode TLPs.

The effect of various environmental statistics on the ζ contours may be estimated by computing the "ultimate" asymptotic performance, ζ_U, using the simple arithmetic involved in Equation 72, and using the approximation $\zeta \cong \zeta_U$. When the modes are weakly coupled, more accurate estimates are obtainable by computing a linear sum of the ζ's of the constituent one-mode processes (Equation 44).

The numerical example suggests that the RC-circuit approximation, together with the weak-coupling approximation, provides a good technique of synthesizing train-work schedules for many two-mode TLPs in which the work ratio is greater than unity.

Equation 111 is a useful formula for estimating the effect of ζ_L, ζ, ζ_F, ξ_w, and ξ_r on the work ratio. Let us define a "good compromise" choice of $\hat{\zeta}_L$ as one which is not so small that ζ_L is too close to ζ_F and at the same time is not so large that the work ratio is made very small by the factor $(\hat{\zeta}_L^{-1} - 1)$ in Equation 111. Intuitively we see that a good compromise choice of $\hat{\zeta}_L$ occurs at the knee of the function

$$f(\hat{\zeta}_L) = \frac{1}{\hat{\zeta}_L} - 1$$

i.e., at $\hat{\zeta}_L = 0.5$. Thus a good compromise choice of ζ_L seems to be

$$\zeta_L = \frac{1}{2} (\zeta + \zeta_F)$$

In control theory, adaptive processes are commonly analyzed by differential equations. In such analyses, the dynamics of systems with fast plant variations have not been satisfactorily understood, and systems with slow plant variations have yielded only to approximate analysis. The present approach permits an exact analysis of the dynamic behavior of both slowly and rapidly perturbed systems. The following sacrifice, however, is made in the use of Markov chains: The results of the analysis are probabilistic, while the results of the differential equation analysis are deterministic. This sacrifice, however, may be put to use if we allow the probabilistic features of the Markov chain model to express our ignorance of the plant and/or its environment.

A worth-while future project would be to show how our ignorance of a deterministic plant and/or its deterministic environment may be expressed as transition probabilities in a Markov chain model.

51

The problem of modeling adaptive processes, i.e., the problem of finding a model that will adequately describe real adaptive processes, is of major importance in this research. (An approach toward this problem is sketched on page 47.) So far our approach has been to gain an understanding of the relation between specific feedback policies — particularly the simple incremental feedback policy — and the adaptation characteristics of a certain class of stochastic processes. The framework of analysis has been Markov chains. A specific application of Markov chains to adaptive signal detection has been demonstrated. In the future we hope to demonstrate the use of Markov chain models for other specific processes in the life sciences and engineering. Models more sophisticated than Markov chains will also be investigated, and specific applications demonstrated.

Another useful future project is the investigation of more sophisticated feedback policies in TLPs. For example, in one-mode TLPs, an improved feedback policy would gradually reduce the size of the threshold increment as a function of time, finally settling on the optimum threshold when the increment is zero. In two-mode TLPs, an improved feedback policy would gradually reduce the size of the threshold increment not to zero but to some small value dependent on a finite history of the incoming signals. It would be interesting to compare the effectiveness of these more complicated feedback policies to the more elementary policies in which the size of the increment remains fixed.

Another useful future project would be an investigation of working-phase feedback for TLPs. This type of feedback involves threshold adjustments based only on the guesses made during the working phase. These guesses would have a nonzero probability of error, but could still be useful in adjusting the threshold, provided the observer in the TLP model knows that the channel may be in one of, say, N modes. Such a situation may occur inadvertently in certain discrimination learning experiments. A knowledge of the effects of working-phase feedback on adaptive behavior will help the experimenter recognize this possibility when it occurs.

Where is this research leading? We feel it leads to the following two situations:

1. When we have available a good theory of adaptive processes, we shall be able to do the following when we encounter an unfamiliar plant to which we would like to tie a feedback policy to enhance the plant's adaptation characteristics: First, we shall construct a model of the plant — a zero-memory statistical model, a Markov chain model, or some other appropriate model. Then our knowledge of the open-loop properties of this model, in addition to our understanding of the effect of various feedback policies on the adaptation characteristics of the model, will enable us to choose a feedback policy that will yield a satisfactory performance of the closed-loop process — taking into consideration our range of ignorance of the expected environments and the unreliability of the internal structure of the plant.

In other words, if we can describe our range of ignorance of the statistical parameters of a given trainee and his environment, we shall be able to find a simple reinforcement strategy that will optimize the learning process of this trainee.

2. Eventually we shall be able to examine certain features of the open-loop and closed-loop performance of an adaptive process, and from these features decide on a reasonably simple model of the process, including a description of an implicit feedback policy that may be hidden inside the process and therefore not directly observable. From such a model we shall be able to predict the transient and asymptotic performance of the process under a variety of environmental conditions and variations of internal structure.

REFERENCES

1. J. Sklansky, "Adaptation and Feedback," *Discrete Adaptive Processes*, edited by J. Sklansky, Institute of Electrical and Electronics Engineers, New York, N. Y., pp. 1-5, June 1962.

2. J. Sklansky, "A Markov Chain Model of Adaptive Signal Detection," Contributed Paper Preprints of the 1963 Bionics Symposium, Air Force Systems Command, Wright-Patterson Air Force Base, Ohio, March 1963.

3. E. N. Gilbert, "Capacity of a Burst-Noise Channel," *Bell System Technical Journal*, Vol. 39, pp. 1253-1266, September 1960.

4. W. H. Huggins, "Signal Flow Graphs and Random Signals," *Proc. IRE*, Vol. 45, pp. 74-86, January 1957.

5. R. Bellman, *Introduction to Matrix Analysis*, McGraw-Hill Book Co., Inc., New York, N. Y., 1960.

6. E. I. Jury, *Sampled-Data Control Systems*, Wiley and Sons, Inc., N. Y., 1958.